

2

AD-A277 995



NAVAL POSTGRADUATE SCHOOL Monterey, California



THESIS

DTIC
ELECTE
APR 11 1994
S G D

THE EFFECT OF THERMOMECHANICAL PROCESSING ON MECHANICAL
PROPERTIES OF A CAST 6061 ALUMINUM METAL MATRIX COMPOSITE

by

Werner Fletcher Hoyt

December 1993

Thesis Advisor:

Terry R. McNelley

Approved for public release: Distribution unlimited.

9380 94-10805



9 4 4 8 024

Unclassified

SECURITY CLASSIFICATION OF THIS PAGE

REPORT DOCUMENTATION PAGE				Form Approved OMB No. 0704-0188									
1a. REPORT SECURITY CLASSIFICATION UNCLASSIFIED		1b. RESTRICTIVE MARKINGS											
2a. SECURITY CLASSIFICATION AUTHORITY		3. DISTRIBUTION/AVAILABILITY OF REPORT Approved for public release; distribution unlimited.											
2b. DECLASSIFICATION/DOWNGRADING SCHEDULE													
4. PERFORMING ORGANIZATION REPORT NUMBER(S)		5. MONITORING ORGANIZATION REPORT NUMBER(S)											
6a. NAME OF PERFORMING ORGANIZATION Naval Postgraduate School		6b. OFFICE SYMBOL (If applicable) ME		7a. NAME OF MONITORING ORGANIZATION Naval Postgraduate School									
6c. ADDRESS (City, State, and ZIP Code) Monterey, CA 93943-5000		7b. ADDRESS (City, State, and ZIP Code) Monterey, CA 93943-5000											
8a. NAME OF FUNDING/SPONSORING ORGANIZATION		8b. OFFICE SYMBOL (If applicable)		9. PROCUREMENT INSTRUMENT IDENTIFICATION NUMBER									
8c. ADDRESS (City, State, and ZIP Code)		10. SOURCE OF FUNDING NUMBERS <table border="1"><thead><tr><th>PROGRAM ELEMENT NO.</th><th>PROJECT NO.</th><th>TASK NO.</th><th>WORK UNIT ACCESSION NO.</th></tr></thead><tbody><tr><td colspan="4"> </td></tr></tbody></table>				PROGRAM ELEMENT NO.	PROJECT NO.	TASK NO.	WORK UNIT ACCESSION NO.				
PROGRAM ELEMENT NO.	PROJECT NO.	TASK NO.	WORK UNIT ACCESSION NO.										
11. TITLE (Include Security Classification) THE EFFECT OF THERMOMECHANICAL PROCESSING ON MECHANICAL PROPERTIES OF A CAST 6061 ALUMINUM METAL MATRIX COMPOSITE													
12. PERSONAL AUTHOR(S) Hoyt, Werner Fletcher													
13a. TYPE OF REPORT Thesis		13b. TIME COVERED FROM _____ TO _____		14. DATE OF REPORT (Year,Month,Day) December 1993									
				15. PAGE COUNT 94									
16. SUPPLEMENTARY NOTATION The views expressed in this thesis are those of the author and do not reflect the official policy or position of the Department of Defense or the U.S. Government.													
17. COSATI CODES <table border="1"><thead><tr><th>FIELD</th><th>GROUP</th><th>SUB-GROUP</th></tr></thead><tbody><tr><td colspan="3"> </td></tr></tbody></table>			FIELD	GROUP	SUB-GROUP				18. SUBJECT TERMS (Continue on reverse if necessary and identify by block number) 6061 Al-Al2O3 Composite; Thermomechanical Processing of MMCs; Aluminum - Alumina Composites; Particle Stimulated Nucleation; PSN; Recrystallization; MMCs; Engineered Materials				
FIELD	GROUP	SUB-GROUP											
19. ABSTRACT (Continue on reverse if necessary and identify by block number) Thermomechanical processing was conducted on cast 6061 Al-Al₂O₃ metal matrix composites (MMCs) containing either 10 or 20 volume percent of alumina (Al₂O₃) particles. These materials were provided by DURALCAN-USA, Inc., of San Diego, CA in conjunction with a Cooperative Research and Development Agreement (CRDA) program on ductility enhancement for these MMCs. Processing included isothermal forging and rolling of materials at 500° C, with interpass anneal (IPA) times of 5 or 30 minutes. Isothermal rolling was also accomplished on 1.0 inch thick 6061-T6 Al plate. Processed materials were solution heat treated at temperatures ranging from 480-560° C, and were then age hardened at 160° C. Tensile testing was conducted to evaluate strength and ductility. Homogeneity of the particle distribution was improved by processing for both composites and no microstructural damage was apparent. Lower solution heat treatment temperature provided significant ductility enhancement while the longer IPA time at 500°C had a minor beneficial effect. As the percentage of reinforcement increased, aging time to peak strength decreased; peak strength, and yield strength increased; and ductility decreased. As the solution heat treatment temperature was decreased ductility was enhanced at a cost of peak strength.													
20. DISTRIBUTION/AVAILABILITY OF ABSTRACT <input checked="" type="checkbox"/> UNCLASSIFIED/UNLIMITED <input type="checkbox"/> SAME AS RPT. <input type="checkbox"/> DTIC USERS			21. ABSTRACT SECURITY CLASSIFICATION UNCLASSIFIED										
22a. NAME OF RESPONSIBLE INDIVIDUAL Terry R. McNelley.			22b. TELEPHONE (Include Area Code) 408 656-2589		22c. OFFICE SYMBOL ME/Mc								

DD Form 1473, JUN 86

Previous editions are obsolete.

S/N 0102-LF-014-6603

SECURITY CLASSIFICATION OF THIS PAGE

Unclassified

Approved for public release: Distribution unlimited.

**THE EFFECT OF THERMOMECHANICAL PROCESSING ON MECHANICAL
PROPERTIES OF A CAST 6061 ALUMINUM METAL MATRIX COMPOSITE**

by

Werner Fletcher Hoyt

**Lieutenant Commander, United States Navy
B.S., University of Oklahoma, 1980**

Submitted in partial fulfillment of the
requirements for the degree of

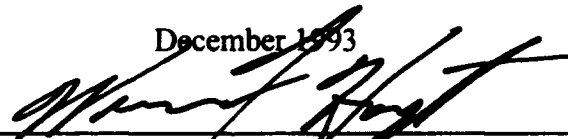
MASTER OF SCIENCE IN MECHANICAL ENGINEERING

from the

NAVAL POSTGRADUATE SCHOOL

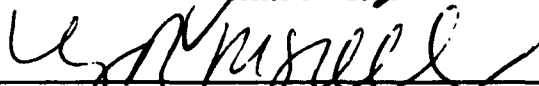
December 1993

Author:



Werner F. Hoyt

Approved by:



Terry R. McNelley, Thesis Advisor



Matthew D. Kelleher, Chairman,

Department of Mechanical Engineering

ABSTRACT

Thermomechanical processing was conducted on cast 6061 Al-Al₂O₃ metal matrix composites (MMCs) containing either 10 or 20 volume percent of alumina (Al₂O₃) particles. These materials were provided by DURALCAN-USA, Inc., of San Diego, CA in conjunction with a Cooperative Research and Development Agreement (CRDA) program on ductility enhancement for these MMCs. Processing included isothermal forging and rolling of materials at 500°C, with interpass anneal (IPA) times of 5 or 30 minutes. Isothermal rolling was also accomplished on 1.0 inch thick 6061-T6 Al plate. Processed materials were solution heat treated at temperatures ranging from 480-560°C, and then were age hardened at 160°C. Tensile testing was conducted to evaluate strength and ductility. Homogeneity of the particle distribution was improved by processing for both composites and no microstructural damage was apparent. Lower solution heat treatment temperature provided significant ductility enhancement while the longer IPA time at 500°C had a minor beneficial effect. As the percentage of reinforcement increased, aging time to peak strength decreased; peak strength, and yield strength increased; and ductility decreased. As the solution heat treatment temperature was decreased ductility was enhanced at a cost of peak strength.

Accession For	
NTIS	CRA&I <input checked="" type="checkbox"/>
DTIC	TAB <input type="checkbox"/>
Unannounced <input type="checkbox"/>	
Justification	
By	
Distribution /	
Availability Codes	
Dist	Avail and/or Special
A-1	

TABLE OF CONTENTS

	Page
I. INTRODUCTION	1
II. BACKGROUND.....	3
A. Studies on Processing of 6061 Al - Al ₂ O ₃ MMCs	3
B. Effects Of The Particle Distribution	5
C. Mechanisms Of Matrix Microstructural Refinement	6
D. Direction Of This Effort.....	9
III. EXPERIMENTAL PROCEDURE	10
A. As Received Material	10
1. Casting.....	10
2. Reference 6061	11
B. Thermomechanical Processing.....	12
1. Solution Treatment.....	13
2. Forging	13
a. Procedure.....	13
b. Calculations.....	14
c. Sample processing schedule	14
3. Rolling.....	15
a. Procedure.....	15
b. Calculations.....	15
C. Tensile Testing	16
1. Machining	16
D. Data Reduction.....	17
E. Age Hardening Study	17
1. Solution Treatment.....	18
2. Aging Temperature	18
3. Composite vs Unreinforced Aluminum	18
F. Optical Microscopy.....	18
1. Polishing Schedule.....	19
2. Anodizing Procedure Of Grain Size Evaluation.	19
IV. RESULTS AND DISCUSSION	22
A. Processing Results.....	22
1. Homogenization Heat Treatment	22
2. Forging	22
3. Rolling.....	22
4. Machining	25
5. Tensile Testing.....	26
B. Optical Microscopy Results	27

1. The Unreinforced 6061 Material.....	27
a. The as-received condition.....	27
b. The as-rolled condition	27
c. Solution heat treated condition.....	29
2. 6061 Matrix With 10 Vol. Pct. Al ₂ O ₃	29
a. Particle redistribution during processing	30
b. Effect of processing on the matrix microstructure	32
3. 6061 Matrix With 20 Vol. Pct. Al ₂ O ₃	37
a. The particle distribution	37
b. Effects of processing on matrix microstructure in the 20 vol. pct. Al ₂ O ₃ MMC.....	39
C. Heat Treatment And Mechanical Properties	45
1. Unreinforced 6061.....	45
2. 6061 - 10 Vol. Pct. Al ₂ O ₃ MMC	48
3. 6061 - 20 Vol. Pct. Al ₂ O ₃ MMC	51
4. Ductility Considerations.....	54
 V. SUMMARY	56
A. Conclusions	56
B. Recommendations For Further Study.....	57
 APPENDIX A: PROCESSING SCHEDULES	58
 APPENDIX B: HARDNESS AND TENSILE TESTING RESULTS	62
 APPENDIX C: GRAPHICAL PRESENTATION OF HARDNESS AND TENSILE TEST DATA FOR 5 MIN. IPA AT 500°C	69
 LIST OF REFERENCES.....	76
 INITIAL DISTRIBUTION LIST.....	79

LIST OF TABLES

TABLE 1. STRENGTH AND DUCTILITY COMPARISONS FOR AGED UNREINFORCED 6061 TO STABILIZED THEN AGED 10 v/o COMPOSITE	4
TABLE 2. PREDICTED GRAIN SIZE (PSN THEORY).....	7
TABLE 3. 6061 AL-10 v/o Al_2O_3 MATRIX COMPOSITION ANALYSIS	11
TABLE 4. 6061 AL-20 v/o Al_2O_3 MATRIX COMPOSITION ANALYSIS	11
TABLE 5. 6061-T6 PLATE COMPOSITION ANALYSIS	11
TABLE 6. PROCESSING SCHEDULE FOR 6061 AL-10 v/o Al_2O_3 (HEAT 1-1169).....	15
TABLE 7. SPECIMEN POLISHING ABRASIVE SCHEDULE.....	20
TABLE 8. PROCESSING SCHEDULE FOR 6061 AL USING 500°C INTERPASS ANNEALS (30 MINUTE S).....	59
TABLE 9. PROCESSING SCHEDULE FOR 6061 AL USING 500°C INTERPASS ANNEALS (5 MINUTES).....	59
TABLE 10. PROCESSING SCHEDULE FOR 6061 AL - 10 v/o Al_2O_3 COMPOSITE USING 500°C INTERPASS ANNEALS (30 MINUTES) (HEAT 1-1169).....	60
TABLE 11. PROCESSING SCHEDULE FOR 6061 AL - 10 v/o Al_2O_3 COMPOSITE USING 500°C INTERPASS ANNEALS (5 MINUTES) (HEAT 1-1169).....	60
TABLE 12. PROCESSING SCHEDULE FOR 6061 AL - 20 v/o Al_2O_3 COMPOSITE USING 500°C INTERPASS ANNEALS (30 MINUTES) (HEAT 1-1095).....	61
TABLE 13. PROCESSING SCHEDULE FOR 6061 AL - 20 v/o Al_2O_3 COMPOSITE USING 500°C INTERPASS ANNEALS (5 MINUTES) (HEAT 1-1095).....	61
TABLE 14. HARDNESS AND TENSILE DATA FOR 6061 AL - 30 MIN. IPA AT 500°C	63
TABLE 15. HARDNESS AND TENSILE DATA FOR 6061 AL - 5 MIN. IPA AT 500°C	64
TABLE 16. HARDNESS AND TENSILE DATA FOR 6061 AL - 10 v/o Al_2O_3 30 MIN. IPA AT 500°C.....	65
TABLE 17. HARDNESS AND TENSILE DATA FOR 6061 AL - 10 v/o Al_2O_3 5 MIN. IPA AT 500°C.....	66
TABLE 18. HARDNESS AND TENSILE DATA FOR 6061 AL - 20 v/o Al_2O_3 30 MIN. IPA AT 500°C.....	67
TABLE 19. HARDNESS AND TENSILE DATA FOR 6061 AL - 20 v/o Al_2O_3 5 MIN. IPA AT 500°C.....	68

LIST OF FIGURES

	Page
Figure 1. Grain size predicted on basis of particle stimulated nucleation of recrystallization.....	8
Figure 2. Critical temperature below which stresses will accumulate at particles for the constant strain rates (sec^{-1})	9
Figure 3. Material provided by DURALCAN-USA	10
Figure 4. Material processing and evaluation flowpath	12
Figure 5. Heated-platen press (forge) arrangement.....	13
Figure 6. Tensile Test Specimen Drawing (All dimensions are in inches)	17
Figure 7. Anodizing configuration.....	21
Figure 8. As-forged billet of 6061 Al - 10 vol. pct. Al_2O_3 with severe longitudinal cracking for an upset forging rate of 0.07 to 0.10 in/sec.	23
Figure 9. As-forged billet of 6061 Al - 10 vol. pct. Al_2O_3 with only traces of longitudinal cracking following use of an upset forging rate of 0.02 to 0.025 in/sec	24
Figure 10. A rolled billet of 6061 Al - 10 vol. pct. Al_2O_3 exhibiting severe edge cracking. This billet had been scarfed prior to machining with approximately 36% wastage.....	25
Figure 11. Rolled billet of 6061 Al - 10 vol. pct Al_2O_3 showing minor edge cracking. The billet had been scarfed prior to rolling (with ~30 % wastage) and prior to machining (with ~5 to 10% additional wastage).....	25
Figure 12. Schematic detail of extensometer contact point with the tensile coupon illustrating the stress concentration point	26
Figure 13. As-received 6061 Al-T6 plate, illustrating the elongated grain structure (grains $\approx 1\text{mm}$ in length). The structure also shows inclusions aligned with the rolling direction.....	28

Figure 14. The as-received 6061 material illustrating the microstructure after the final rolling pass (true strain of 2.4).....	28
Figure 15. The rolled and solution heat treated 6061 (5 minutes IPA time) illustrating the microstructure after solution treatment 480°C for 1 hr.....	29
Figure 16. A micrograph of the as-cast 6061 Al - 10 vol. pct. Al ₂ O ₃ composite illustrating the inhomogeneity of the particle distribution. Polished (not etched)	31
Figure 17. The forged 6061 - 10 vol. pct. Al ₂ O ₃ MMC illustrating redistribution of the particles during straining. Polished (not etched).....	31
Figure 18. The as-rolled 6061 Al - 10 vol. pct. Al ₂ O ₃ composite illustrating further redistribution of the particles during rolling. Polished (not etched).....	32
Figure 19. The as-cast 6061 Al- 10 vol. pct. Al ₂ O ₃ composite illustrating a coarse and irregular grain structure.....	34
Figure 20. As-cast and homogenized 6061 Al - 10 vol. pct. Al ₂ O ₃ composite illustrating the same grain structure and the resolutioning of the Mg ₂ Si.....	34
Figure 21. The forged 6061 Al - 10 vol. pct. Al ₂ O ₃ MMC, illustrating grain refinement of the matrix.....	35
Figure 22. The as-rolled condition for the 6061 Al - 10 vol. pct. Al ₂ O ₃ material illustrating distortion by rolling deformation of a previously recrystallized grain structure	35
Figure 23. Reheating of the rolled 6061 Al - 10 vol. pct. Al ₂ O ₃ material for 5 minutes at 500°C results in PSN of recrystallization	36
Figure 24. The effect of solution heat treatment for one hour at 560°C on the rolled 6061 Al - 10 vol. pct. Al ₂ O ₃ composite, showing PSN of recrystallization. The particle spacing appears to be the controlling factor in grain size	36

Figure 25. The particle distribution in the as-cast 6061 Al - 20 vol. pct. Al_2O_3 composite illustrating greater homogeneity than apparent in the 10 vol. pct. Al_2O_3 material (see Figure 16). As polished (not etched).....	38
Figure 26. The forged 6061 Al - 20 vol. pct. Al_2O_3 MMC, illustrating improved homogeneity of the particle distribution. As-polished (not etched).....	38
Figure 27. The rolled 6061 Al - 20 vol. pct. Al_2O_3 material showing an essentially homogeneous particle distribution but with the alignment of particles in the rolling direction. As polished (not etched).....	39
Figure 28. The as-cast 6061 Al - 20 vol. pct. Al_2O_3 composite showing coarse, irregular grains. Anodized and examined under crossed polars.....	40
Figure 29. The as-cast and homogenized 6061 Al - 20 vol. pct. Al_2O_3 composite illustrating the same coarse and irregular grain structure as in the as-cast condition. Anodized and examined under crossed polars	41
Figure 30. As-forged 6061 Al - 20 vol. pct Al_2O_3 composite illustrating PSN of recrystallization in the grain structure on completion of forging.....	42
Figure 31. As-rolled 6061 Al - 20 v/o Al_2O_3 composite illustrating deformation by rolling of the previously recrystallized grain structure.....	42
Figure 32. Rolled 6061 Al - 20 v/o Al_2O_3 composite illustrating complete PSN of recrystallization after reheating of a coupon for 5 min. at 500°C	43
Figure 33. The microstructure of a rolled and solution heat treated 6061 Al - 20 vol. pct. Al_2O_3 composite illustrating complete recrystallization via PSN. Solution heat treatment was for one hour at 560°C. Anodized and viewed under crossed polars.....	44
Figure 34. Plot of elongation versus aging time for unreinforced 6061 material processed utilizing a 30 min. IPA during rolling at 500°C. Data are included for four different solution heat treatment temperatures	46

Figure 35. Plot of yield strength versus aging time for unreinforced 6061 material processed utilizing a 30 min. IPA during rolling at 500°C. Data are included for four different solution heat treatment temperatures	46
Figure 36. Plot of ultimate tensile strength versus aging time for unreinforced 6061 material processed utilizing a 30 min. IPA during rolling at 500°C. Data are included for four different solution heat treatment temperatures.....	47
Figure 37. Plot of hardness versus aging time for unreinforced 6061 material processed utilizing a 30 min. IPA during rolling at 500°C. Data are included for four different solution heat treatment temperatures	47
Figure 38. Plot of elongation versus aging time for 6061 Al - 10 vol. pct. Al ₂ O ₃ material processed utilizing a 30 min. IPA during rolling at 500°C. Data are included for four different solution heat treatment temperatures	49
Figure 39. Plot of yield strength versus aging time for 6061 Al - 10 vol. pct. Al ₂ O ₃ material processed utilizing a 30 min. IPA during rolling at 500°C. Data are included for four different solution heat treatment temperatures	50
Figure 40. Plot of ultimate tensile strength versus aging time for 6061 Al - 10 vol. pct. Al ₂ O ₃ material processed utilizing a 30 min. IPA during rolling at 500°C. Data are included for four different solution heat treatment temperatures.....	50
Figure 41. Plot of hardness versus aging time for 6061 Al - 10 vol. pct. Al ₂ O ₃ material processed utilizing a 30 min. IPA during rolling at 500°C. Data are included for four different solution heat treatment temperatures	51
Figure 42. Plot of elongation versus aging time for 6061 Al - 20 vol. pct. Al ₂ O ₃ material processed utilizing a 30 min. IPA during rolling at 500°C. Data are included for three different solution heat treatment temperatures	52
Figure 43. Plot of yield strength versus aging time for 6061 Al - 20 vol. pct. Al ₂ O ₃ material processed utilizing a 30 min. IPA during rolling at 500°C. Data are included for three different solution heat treatment temperatures	53

Figure 44. Plot of ultimate tensile strength versus aging time for 6061 Al - 20 vol. pct. Al_2O_3 material processed utilizing a 30 min. IPA during rolling at 500°C. Data are included for three different solution heat treatment temperatures.....	53
Figure 45. Plot of hardness versus aging time for 6061 Al - 20 vol. pct. Al_2O_3 material processed utilizing a 30 min. IPA during rolling at 500°C. Data are included for three different solution heat treatment temperatures	54
Figure 46. Plot of elongation versus aging time for unreinforced 6061 material processed utilizing a 5 min. IPA during rolling at 500°C. Data are included for four different solution heat treatment temperatures	70
Figure 47. Plot of yield strength versus aging time for unreinforced 6061 material processed utilizing a 5 min. IPA during rolling at 500°C. Data are included for four different solution heat treatment temperatures	70
Figure 48. Plot of ultimate tensile strength versus aging time for unreinforced 6061 material processed utilizing a 5 min. IPA during rolling at 500°C. Data are included for four different solution heat treatment temperatures	71
Figure 49. Plot of hardness versus aging time for unreinforced 6061 material processed utilizing a 5 min. IPA during rolling at 500°C. Data are included for four different solution heat treatment temperatures	71
Figure 50. Plot of elongation versus aging time for 6061 Al - 10 vol. pct. Al_2O_3 material processed utilizing a 5 min. IPA during rolling at 500°C. Data are included for four different solution heat treatment temperatures	72
Figure 51. Plot of yield strength versus aging time for 6061 Al - 10 vol. pct. Al_2O_3 material processed utilizing a 5 min. IPA during rolling at 500°C. Data are included for four different solution heat treatment temperatures	72

Figure 52. Plot of ultimate tensile strength versus aging time for 6061 Al - 10 vol. pct. Al_2O_3 material processed utilizing a 5 min. IPA during rolling at 500°C. Data are included for four different solution heat treatment temperatures.....	73
Figure 53. Plot of hardness versus aging time for 6061 Al - 10 vol. pct. Al_2O_3 material processed utilizing a 5 min. IPA during rolling at 500°C. Data are included for four different solution heat treatment temperatures	73
Figure 54. Plot of elongation versus aging time for 6061 Al - 20 vol. pct. Al_2O_3 material processed utilizing a 5 min. IPA during rolling at 500°C. Data are included for four different solution heat treatment temperatures	74
Figure 55. Plot of yield strength versus aging time for 6061 Al - 20 vol. pct. Al_2O_3 material processed utilizing a 5 min. IPA during rolling at 500°C. Data are included for four different solution heat treatment temperatures	74
Figure 56. Plot of ultimate tensile strength versus aging time for 6061 Al - 20 vol. pct. Al_2O_3 material processed utilizing a 5 min. IPA during rolling at 500°C. Data are included for four different solution heat treatment temperatures.....	75
Figure 57. Plot of hardness versus aging time for 6061 Al - 20 vol. pct. Al_2O_3 material processed utilizing a 5 min. IPA during rolling at 500°C. Data are included for four different solution heat treatment temperatures	75

ACKNOWLEDGEMENTS

I would like to thank Dr. Terry R. McNelley for his assistance and guidance through the course of this research. My most sincere thanks go to my beautiful wife, Misoon and my lovely daughters, Ella and Johanna for their love, understanding and support without which this entire work would not have been possible. My thanks to Doug Shelton for assistance with laboratory equipment setup and general help with equipment. I would also like to thank DURALCAN-USA for funding this work and provision of materials as well as Mr. William Dixon for his encouragement and support.

I. INTRODUCTION

The engineered materials area is now expanding rapidly with new developments. Engineered materials are those that have had their properties (e.g., stiffness, strength, ductility or wear resistance) tailored to a desired condition during manufacturing. Aluminum alloys reinforced with either alumina (Al_2O_3) or silicon carbide (SiC) particles are engineered materials. In the past these materials have been produced by powder metallurgy methods. More recently, DURALCAN of San Diego, CA has pioneered ingot metallurgy methods to produce Aluminum-based, particle-reinforced metal matrix composites (MMCs). The process involves melting the matrix alloy and stirring in the particulate reinforcement to create the composite which is then cast either into a useable form or to provide ingot material for subsequent deformation processing. An advantage of this production route is the potentially large size of ingots which can be made. Thus, there is the potential for low cost, high volume production of these materials.

Until now MMCs, whether manufactured by powder or ingot processes, have lacked sufficient ductility for many engineering applications. Although they have many desirable properties (high stiffness, high wear resistance, and high strength) their lack of ductility has prevented their application in many end uses. One category of applications is those which are deflection limited and thus require a high ratio of modulus of elasticity, E , to density, ρ . An example is an extruded tubular automotive drive shaft. Increasing the E/ρ ratio increases the rotational speed prior to the onset of transverse vibration due to gravitational effects. A possible military application would be materials for lightweight armor vehicles. An improved E/ρ ratio would reduce vehicle weight if suitable ballistic impact characteristics can be achieved.

Research on the thermomechanical processing (TMP) of cast MMC materials followed efforts at the Naval Postgraduate School on grain refinement and superplasticity in Al alloys [Refs. 2-9]. Initial studies involved application of additional TMP to

extruded MMC materials. This work demonstrated that composite ductility could be enhanced with little or no strength decrease by such processing [Refs. 10-17]. Subsequent interest by DURALCAN has resulted in the present research effort. This investigation seeks to expand on the previous work as part of a Cooperative Research and Development Agreement (CRDA) [Ref. 1] to enhance the ductility of current 6061 Al - Al_2O_3 metal matrix composites for the purpose of manufacturing extruded and rolled products. The MMC's of interest here contain either 10 vol. pct of $12.5\mu\text{m}$ Al_2O_3 or 20 vol. pct. of $19.0\mu\text{m}$ Al_2O_3 particles (mean diameters).

II. BACKGROUND

The factors which influence the ductility of particle-reinforced MMCs are not fully understood. The relationship between strength and ductility for the unreinforced matrix is complicated by the interaction of the added reinforcement particles with the matrix. This interaction is affected by factors such as the particle size and shape, the particle distribution, interfacial phenomena, mismatch of particle and matrix thermal expansion coefficients, and damage to particles during processing. Thus, a complete theory of deformation and fracture for particle-reinforced MMC materials remains to be developed and will require both experimental and theoretical approaches. Indeed, most of these factors are influenced by processing history and therefore the evolution of MMC microstructure and properties during processing requires detailed study.

A. STUDIES ON PROCESSING OF 6061 AL - Al_2O_3 MMCS

Initial work on 6061 Al - Al_2O_3 materials in this laboratory [Ref. 10-17] adapted TMP methods developed in work on processing of superplastic Al-Mg alloys [Ref. 2-9] for the rolling of these MMCs. The rolling was accomplished on material supplied in an initially extruded condition and thus constituted additional TMP. This work demonstrated that the additional processing reduced the extent of banding in the particle distribution and enhanced the ductility of the processed material. Subsequent studies examined the effects of processing on the matrix microstructure. It was shown that matrix grain refinement could be accomplished by particle-stimulated nucleation (PSN) of recrystallization for suitably chosen processing conditions [Ref. 10].

Eastwood [Ref. 17] examined subsequent heat treatment of the processed MMC materials. The use of reduced solution heat treatment (SHT) temperatures was investigated as a means of retaining grain refinement achieved in prior processing. It was shown that exceptional ductility could be obtained in heat treated material but at the cost of some strength. Data for unreinforced 6061 are compared in Table 1 to data for the processed and heat treated composite [Ref. 17]. The data for unreinforced 6061 corresponds to SHT at 560°C followed by aging for 18 hrs. at 160°C to achieve a T6 temper. The composite was given a stabilizing heat treatment consisting of a soak at 500°C rather than a full SHT at a higher temperature. This was followed by various aging treatments at 160°C as indicated in Table 1.

TABLE 1. STRENGTH AND DUCTILITY COMPARISONS FOR AGED UNREINFORCED 6061 TO STABILIZED THEN AGED 10 V/O COMPOSITE.

Material	Time (hr)	Yield Strength (MPa)	UTS (MPa)	Percent Elongation (%)
Unreinforced 6061 Aged T6	18	276	310	17.2
Stabilized and Aged Composite	8.3	205	263	17
Stabilized and Aged Composite	12.5	278	343	14

The data indicate that the composite can be heat treated to achieve the same ductility as the unreinforced matrix alloy (17 pct. elongation to failure) but at a lower strength. If the processed composite is aged to attain the same strength as the unreinforced matrix a somewhat lower ductility, 14 pct. elongation to failure, is obtained. This latter MMC ductility is still well in excess of typical values reported for such materials. Indeed, higher strengths with lower ductilities were obtained in the MMC upon full SHT of the MMC. Eastwood [Ref. 17] considered a single soaking temperature and conducted one test only

for each final heat treatment condition. This work will examine a wider range of heat treating and mechanical testing conditions in order to achieve a better picture of the strength/ductility combinations attainable in this material.

B. EFFECTS OF THE PARTICLE DISTRIBUTION

The homogeneity of the particle distribution in Al-matrix MMC materials has been recognized as a significant factor in composite ductility. The ductility improvements noted in previous work in this laboratory [Ref. 10-17] have been attributed in part to homogenization of the Al_2O_3 particle distribution. Particles located in bands present in extruded material were redistributed during processing although true strains ≥ 4.0 were necessary to achieve homogeneous distributions. As the particle distribution became progressively homogenized the matrix grain structures were refined by PSN of recrystallization and this was proposed to be an additional factor in composite ductility [Ref. 10].

Osman, Lewandowski and Hunt and Lewandowski et al. [Ref. 18,19] have also conducted experiments to assess the influence of particle distributions on MMC mechanical properties. They concluded that composite ductility was controlled by failure mechanisms initiated within particle clusters for inhomogeneous particle distributions. As the materials were processed to homogenize particle distributions MMC failure began to be dominated by processes occurring in the matrix and composite ductility was seen to improve.

Through analysis of finite element models of MMC deformation, Lorca, et al. [Ref. 20] identified two factors limiting composite ductility. The first limitation is due to void nucleation at sharp corners of the reinforcement particles in association with strain concentrations at such locations. The second limitation was acceleration of void formation within particle clusters in the matrix. These analyses considered good

particle/matrix bonding and it was noted that debonding in association with stress concentrations would further accelerate void formation and further limit composite ductility.

Homogeneity of particle distributions is generally assessed qualitatively. Microstructures representing various stages of processing are often compared and particle distributions are deemed more or less homogenous in a relative sense. The absence of a quantitative measure of homogeneity for randomly distributed particles hampers our ability to assess the particle distributions of microstructures. The characterization of particle distributions in these Al - Al₂O₃ materials is being examined in a concurrent study by Longenecker [Ref. 21].

C. MECHANISMS OF MATRIX MICROSTRUCTURAL REFINEMENT

Investigations [Ref. 10-11] of matrix microstructural evolution during TMP of 6061 Al - Al₂O₃ materials have shown that PSN of recrystallization may occur for appropriate processing conditions. The associated grain refinement was suggested [Ref. 10-11] to be a significant factor in ductility enhancement due to TMP for these conditions. The theory of PSN was developed from studies on recrystallization due to dilute dispersions of particles in single crystals deformed at ordinary temperatures [Ref. 22]. Subsequent work has considered the influence of deformation temperature [Ref. 24-25] and application of the theory to processed MMC materials.

There are two essential prerequisites for PSN [Ref. 22, 24] in deformed particle containing materials. The first is the presence of local lattice rotations within the deformation zones surrounding particles, and the second is sufficient strain energy stored within the deformation zone to allow growth of an embryo of a recrystallized grain. Bigger particles provide larger deformation zones for a given strain and so conditions for recrystallization are achieved more readily at larger particles. Thus, with smaller particles

more strain is required to initiate recrystallization and there may be a practical lower limit of $\approx 1.0\mu\text{m}$ for particles to serve as nucleation sites in deformed Al alloys [Ref. 22-24]. If all particles in a dispersion serve as nucleation sites the grain size can be estimated [Ref. 24] from the relationship

$$D_{PSN} = \frac{d_p}{f_v^{1/3}} \quad (1)$$

where D_{PSN} is the recrystallized grain size, d_p is the particle size and f_v is the volume fraction of particles. The results of this prediction are summarized in Table 2 and Figure 1 for the materials of interest in this work.

TABLE 2 -PREDICTED GRAIN SIZE (PSN THEORY).

Volume Fraction	Particle Diameter	Predicted Grain Size
0.10	12.5 μ	26 μ
0.20	19 μ	41 μ

The processing in this work involves rolling at elevated temperatures. At sufficiently high temperatures, recovery by dislocation climb may preclude formation of lattice rotations within deformation zones at particles. This problem has been addressed by Humphreys and Kalu [Ref. 24] who have provided an equation to estimate the critical strain rate $\dot{\epsilon}_c$ above which deformation zones are expected to form during elevated temperature straining:

$$\dot{\epsilon}_c = \frac{K_1}{Td_p^2} \exp\left(-\frac{Q_v}{RT}\right) + \frac{K_2}{Td_p^3} \exp\left(-\frac{Q_b}{RT}\right) \quad (2)$$

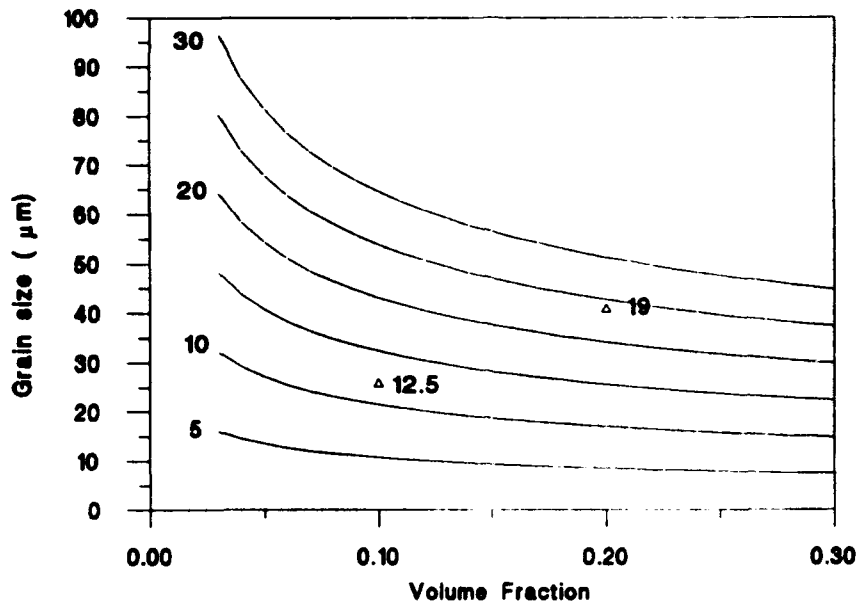


Figure 1. Grain size predicted on basis of particle stimulated nucleation of recrystallization.

where K_1 and K_2 are constants, R and T have the usual meaning, Q_v is the activation energy for volume diffusion, and Q_b is the activation energy for diffusion in the particle/matrix interface. Usually, the second term dominates [Ref. 24] and

$$\dot{\epsilon} \cong \frac{K_2}{Td_p^3} \exp\left(-\frac{Q_b}{RT}\right) \quad (3)$$

and this has been shown to describe the conditions for the onset of PSN in particle-containing Al-Mg materials [Ref. 2, 23-24]. For appropriate values for Q_b and K_2 [Ref. 2, 23-24], Equation 3 may be plotted to provide estimates of the relationship between strain rate and temperature for which PSN is expected in the 6061 Al - Al_2O_3 materials of this research. These are shown in Figure 2. Each curve defines the

temperature as a function of particle size below which PSN is expected at the indicated strain rate.

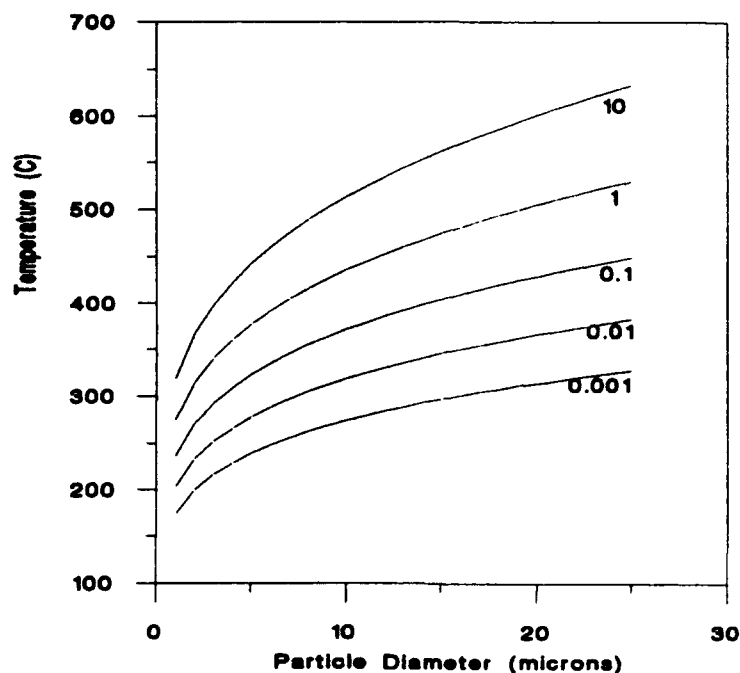


Figure 2. Critical temperature below which stresses will accumulate at particles for the constant strain rates (sec^{-1})

D. DIRECTION OF THIS EFFORT

This research will first consider procedures for the forging and rolling of cast 6061 Al - Al_2O_3 materials containing either 10 or 20 volume percent of particles. The TMP methods will be adapted from those previously employed in processing of superplastic Al-Mg materials [Ref. 2-9]. Evolution of both particle distributions and matrix microstructures will be observed at various stages of the processing and attention will be given to possible particle damage during processing. Mechanical properties of the processed materials will be assessed and correlated with microstructure.

III. EXPERIMENTAL PROCEDURE

A. AS RECEIVED MATERIAL

1. Casting

The Al 6061 10 v/o or 20 v/o Al_2O_3 billets provided by the manufacturer, DURALCAN-USA of San Diego, CA, were sectioned and machined from a 7.0 in (17.8 cm) diameter by 20 in (50.8 cm) long direct chill casting by the manufacturer. The billet dimensions were 1.75 in x 2.0 in x 3.0 in (44 mm x 51 mm x 76 mm). The two inch dimension was parallel to the axis of the casting (Figure 3).

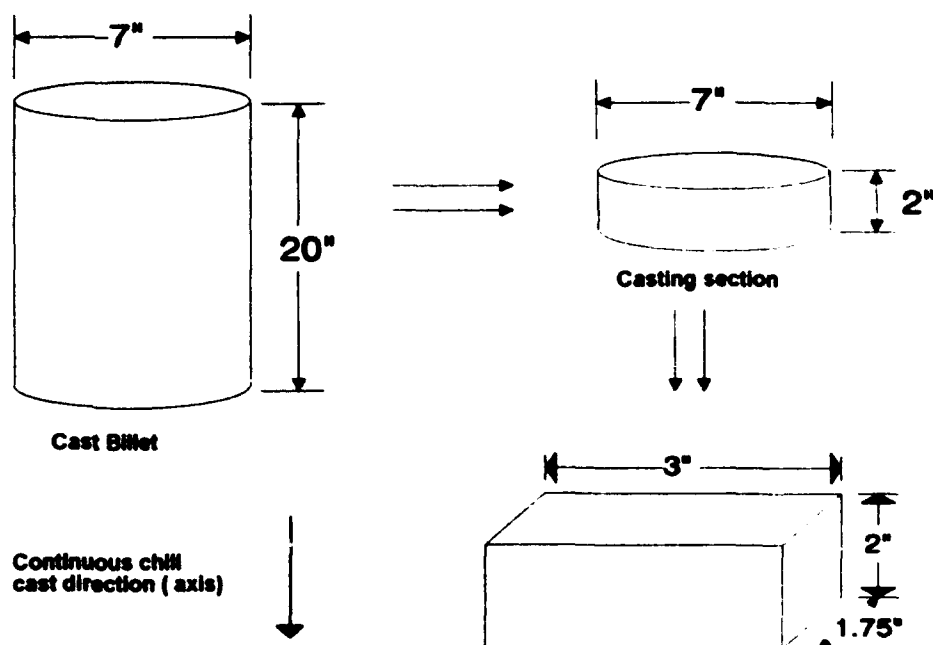


Figure 3. Material provided by DURALCAN-USA

The 6061 Al - Al_2O_3 MMCs provided by DURALCAN contained either 10 or 20 volume percent of alumina particles with mean particle diameters of 12.5 μm or 19 μm ,

respectively. The matrix compositions were provided by DURALCAN [Ref. 26] and are given in Tables 3 and 4.

TABLE 3. 6061 AL-10 V/O AL₂O₃ MATRIX COMPOSITION ANALYSIS

Si	Fe	Cu	Mn	Mg	Cr	Zn	Ti	Be	Sr
0.57	0.07	0.25	<0.01	1.05	0.12	<0.01	0.01	---	---

TABLE 4. 6061 AL-20 V/O AL₂O₃ MATRIX COMPOSITION ANALYSIS

Si	Fe	Cu	Mn	Mg	Cr	Zn	Ti	Be	Sr
0.05	0.05	0.27	<0.01	1.00	0.12	0.01	0.01	---	---

2. Reference 6061

The 6061-T6 Aluminum plate used to provide data applicable to the unreinforced matrix was also tested by DURALCAN [Ref. 27] and composition data is provided in Table 5.

TABLE 5. 6061-T6 PLATE COMPOSITION ANALYSIS

Si	Fe	Cu	Mn	Mg	Cr	Zn	Ti	Be	Sr
0.67	0.48	0.22	0.11	1.03	0.17	0.14	0.03	0.0002	---

Samples of the as received cast ingot castings were sectioned for investigation of the particle distribution and grain structure.

B. THERMOMECHANICAL PROCESSING

The thermomechanical process (TMP) and subsequent test plan are illustrated in Figure 4.

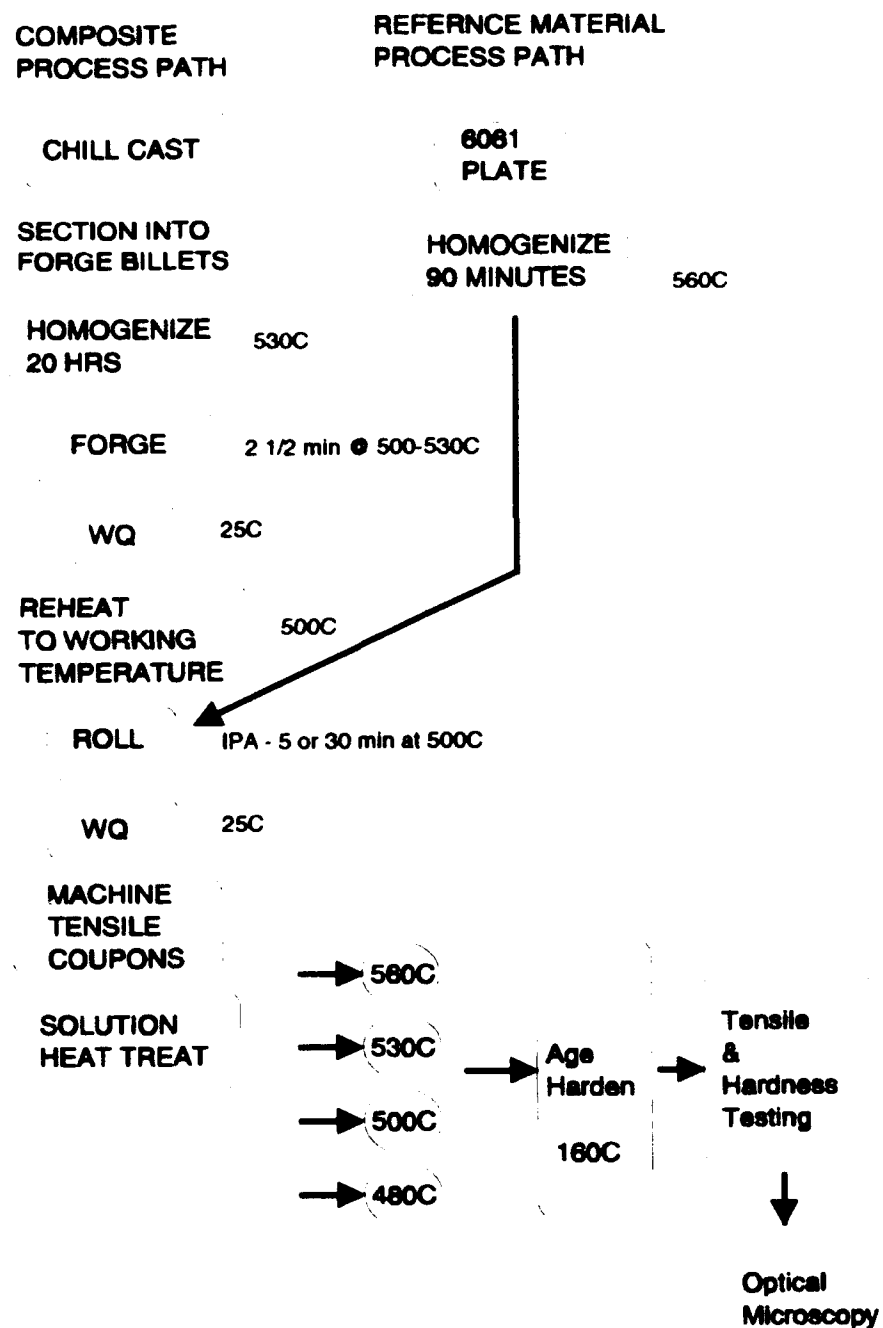


Figure 4. Material processing and evaluation flowpath

1. Solution Treatment

Billets of the 10 v/o or 20 v/o composite were solutionized 20 hrs at 530°C in order to insure homogeneity prior to forging using a Lindberg electric laboratory box type furnace. The 6061-T6 plate was solutionized 90 minutes at 560°C to eliminate the effects of the aging treatment on the material prior to rolling.

2. Forging

a. Procedure

The MMC billets were removed from the solution treatment furnace and were placed in a heated-platen press. They were upset forged from a an initial thickness of 3.0 inch (76mm) to a final thickness of 1.0 inch (25 mm) using gage blocks as press stops (Figure 5).

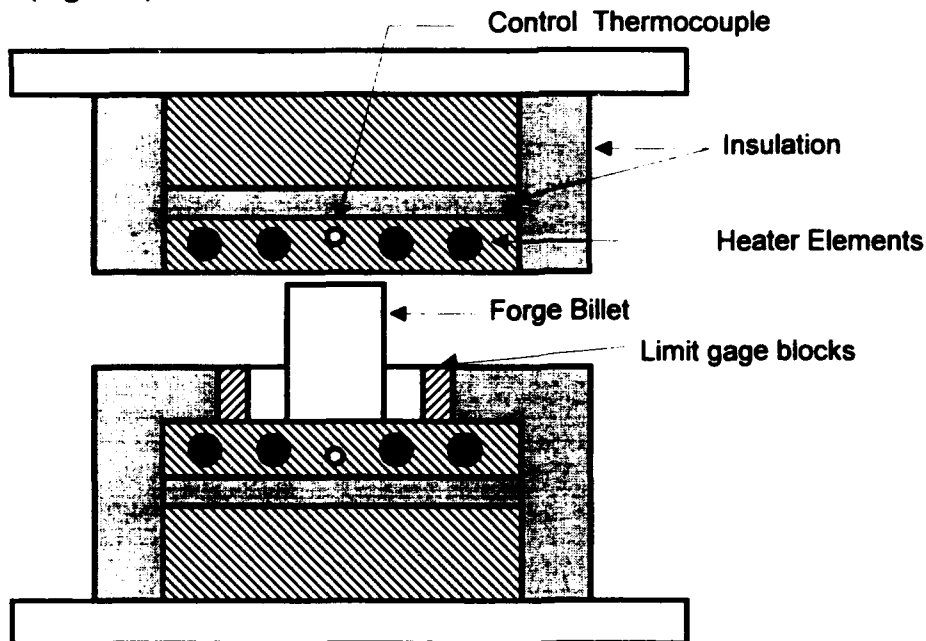


Figure 5. Heated-platen press (forge) arrangement.

Pressing duration was 150 sec \pm 10 sec, corresponding to a forging rate of \sim 0.013 in/sec (0.33 mm/sec). Platen temperatures were controlled at 480 to 500°C and extreme care was given to not exceeding 500°C platen temperatures in order to avoid overtempering of the platen material. Prior to heating the platens were sprayed with silicone lubricant to prevent the forged billet from sticking to either of the platen faces.

b. Calculations

Computations for the forging portion of the processing schedule included the engineering strain, true strain and maximum forging strain rate (Equations 4-6). The engineering strain is given by

$$\epsilon = \frac{T_o - T_f}{T_o} \quad (4)$$

where T_o = the initial thickness and T_f = the final thickness after forging. the true strain is given by

$$\epsilon_{true} = \ln(1 + \epsilon) \quad (5)$$

while the forging strain rate is given by

$$\dot{\epsilon} = \frac{\Delta T / T_f}{\Delta t} \quad (6)$$

where ΔT = is the thickness change and Δt = the total time (sec).

c. Sample processing schedule

Rolling schedule data was processed via a spreadsheet program as illustrated Table 6. A complete set of rolling schedules is presented in Appendix A (Tables 8-13).

TABLE 6. PROCESSING SCHEDULE FOR 6061 AL-10 V/O AL₂O₃ (HEAT 1-1169)

Roll #	To (in)	Tf (in)	Mill Gap Setting (in)	Mill Deflect (in)	strain rate (1/sec)	e (in/in)
1	1.010	0.925	0.900	0.025	0.867	0.088
2	0.925	0.806	0.790	0.016	1.140	0.138
3	0.806	0.702	0.680	0.022	1.224	0.138
4	0.702	0.592	0.570	0.022	1.462	0.170
5	0.592	0.474	0.460	0.014	1.829	0.222
6	0.474	0.375	0.350	0.025	2.102	0.234
7	0.375	0.282	0.265	0.017	2.622	0.285
8	0.282	0.220	0.195	0.025	2.810	0.248
9	0.220	0.169	0.140	0.029	3.285	0.264
10	0.169	0.124	0.100	0.024	4.082	0.310
11	0.124	0.093	0.070	0.023	4.582	0.288
Total					Rolling Strain	
					2.385	
					max e	
Forging					(1/sec)	
1	3	1.01				1.089
					Total Strain	
					3.474	

3. Rolling

a. Procedure

The same thermomechanical process (TMP) schedules were utilized for the 10 and 20 volume percent composites and for the unreinforced 6061-T6 plate. A 500°C interpass anneal temperature was used for either 5 or 30 minutes of annealing between passes (Table 6).

b. Calculations

Computations for the rolling portion of the processing schedule included the rolling mill deflection (equation 7), the engineering strain (equation 4), the true strain (equation 5), and the average rolling strain rate (equations 8) for each pass.

The mill deflection is

$$\text{Mill_Deflection} = T_{\text{roll_setting}} - T_f. \quad (7)$$

Finally the rolling strain rate [Ref. 28] is given by

$$\dot{\epsilon} = \frac{V_r}{\sqrt{R \cdot h_o}} \sqrt{\left(\epsilon \left(1 + \frac{1}{\epsilon} \right) \right)} \quad (8)$$

where $V_r = 2\pi Rn(\text{in/sec})$, $n = \text{speed of the roller (rev/sec)}$, $R = \text{Roller radius (in)}$, $h_o = T_o = \text{initial sample thickness (in)}$, and $\epsilon = \text{engineering strain defined in eq. (4)}$

C. TENSILE TESTING

Tensile test data obtained from the Instron Model 4705 Tension Tester were processed with a Zenith 286 P.C. and plots of engineering stress vs. engineering strain were obtained from the Instron SERIES IX Materials Testing System program. Test data acquisition rate was two data points per second. The system stored the raw data as load (lbf) and extension (in). Test data was backed up on 360 K 5 1/2" data disks as compressed system files and uncompressed ASCII files to allow for further analysis of the test results. All tests utilized a constant cross head speed of 0.5 mm/min. All tests were conducted at $\approx 20\text{--}25^\circ\text{C}$. The program reports also provided ultimate tensile strength and total strain to fracture.

1. Machining

Tensile test coupons were machined from rolled billets to the dimensions shown in Figure 6. The composite materials were highly abrasive and thus all cutting and machining was accomplished utilizing diamond or cobalt cutting/milling tools.

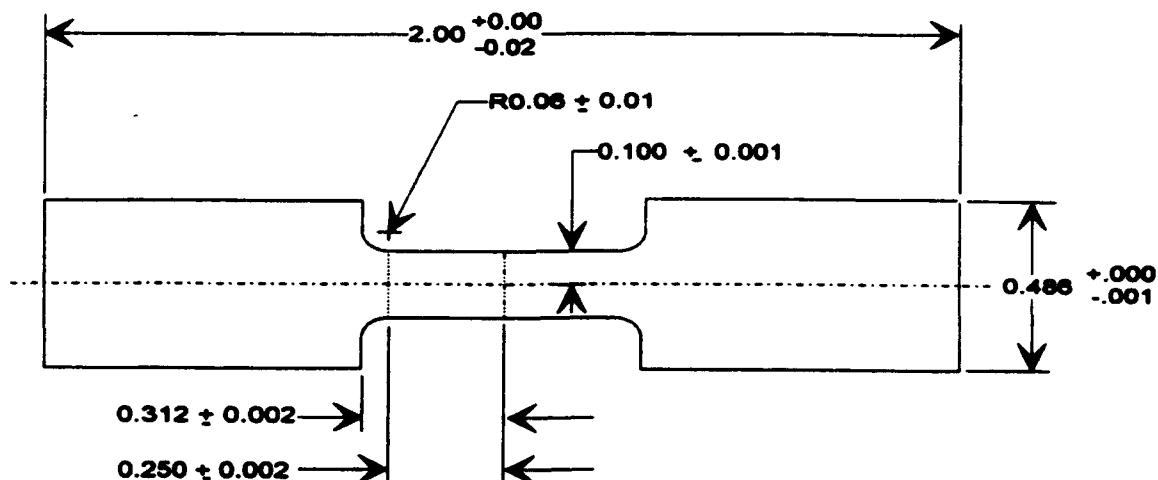


Figure 6. Tensile Test Specimen Drawing (All dimensions are in inches)

D. DATA REDUCTION

Data was converted and exported from the Instron compressed file format into ASCII files. Using Microsoft Word the raw data could be then pasted to Cricket Graph and edited remove data points past peak true stress for the plots of true stress vs true strain. Microsoft Excel was used for all tables and for reduction of the raw hardness data. Graphing of hardness and tensile test data was accomplished in Cricket Graph.

E. AGE HARDENING STUDY

An aging study was conducted to determine the aging response of the materials using hardness as a concurrent measure of the ultimate tensile strength (UTS). The coupon hardness was tested on a Rockwell Hardness Tester (Model Nr 1JR) using the "F" scale (60 kg mass and 1/16" dia ball penetrator). The test coupons were then tested on the Instron. The hardness and tensile test results are graphically represented in the Results and Discussion section and Appendix C while the data tables are contained in Appendix B.

1. Solution Treatment

A portion of sample material was cut from all final rolling passes. On completion of rolling the material was immediately water quenched to preserve it in the as-rolled state prior to sectioning into tensile coupons. Coupons were then solution treated at 560, 530, 500 or 480°C for 1 hour prior to aging.

2. Aging Temperature

The aging temperature of 160°C was selected on the basis of handbook data [Ref. 29] and previous work done by Schaefer [Ref. 13], whose study was conducted at 160°C, and also Eastwood [Ref. 17] who used 160°C as a middle temperature for aging studies.

3. Composite vs. Unreinforced Aluminum

The unreinforced aluminum was processed and aged under the same conditions as the 10 or 20 volume percent composite to provide a control set in order to evaluate the response of the composite materials.

F. OPTICAL MICROSCOPY

Both composite materials and the unreinforced 6061 aluminum were examined with an optical microscope (Zeiss ICM-405 Optical Microscope) to assess particle distribution. Photographs were taken with Polaroid Type T-55 positive/negative film. Samples were anodized and 35 mm photographs were taken with Kodak TMAX 100 B&W film using a Zeiss Photographic Microscope with a vertical eyepiece adapter to a Nikon 35 mm SLR camera. The film was developed at 68°F (20°C) for 13.5 minutes using Microdol Developer and then standard times for stop and fix baths.

1. Polishing Schedule

The polishing schedule utilized by Eastwood [Ref. 17] was revised and adapted for this work to reflect the availability of new grinding equipment (Knuth Rotor Grinders) [Ref. 30]. Standard polishing techniques for optical polishing requires grit size selection to be reduced approx 50 percent at each step. Utilizing this as a basis the schedule summarized in Table 7 was developed.

2. Anodizing Procedure For Grain Size Evaluation.

A Barkers Reagent solution was prepared from 55 ml HBF_4 (48-50% solution), 945 ml distilled water, and 7 gm Boric Acid. Samples were anodized using a DC power supply set at 10 Volts. The sample served as the circuit anode. The negative (black) lead was connected to the metal beaker with magnetic stirring for solution agitation. The samples were placed in an agitated solution for 30 to 40 seconds and then checked at 10 second increments of anodizing in order to obtain the optimum contrast enhancement under cross polars and to prevent over anodizing [Ref. 31]

TABLE 7. SPECIMEN POLISHING ABRASIVE SCHEDULE

Step Number	Polishing Medium	Grit Size	Grit Dia (microns)	Time (min)	Wheel RPM	Comments
1	Carbide paper	230	46	0.5	12" dia 300 rpm	1-5 lbf *
2	Carbide paper	500	30	0.5	12" dia 300 rpm	1-3 lbf *
3	Carbide paper	1000	18	2	12" dia 300 rpm	1-3 lbf *
4	Carbide paper	2400	10	3	12" dia 300 rpm	1-3 lbf *
5	Carbide paper	4000	5	3	12" dia 300 rpm	1-3 lbf *
6	diamond spray w/ Metadi extender chemtex cloth		6	6-9	12" dia 250 rpm	1-3 lbf *
7	diamond spray w/ Metadi extender microcloth		1	6-9	12" dia 250 rpm	1-2 lbf *
8	Collodial Silica microcloth		0.05	1	12" dia Slow spd	1-2 lbf *

* Start at upper pressure and gradually ease off until light pressure is applied at end of stage. For the carbide abrasive paper insure that water flow is adequate to insure sufficient lubrication for best cutting effect.

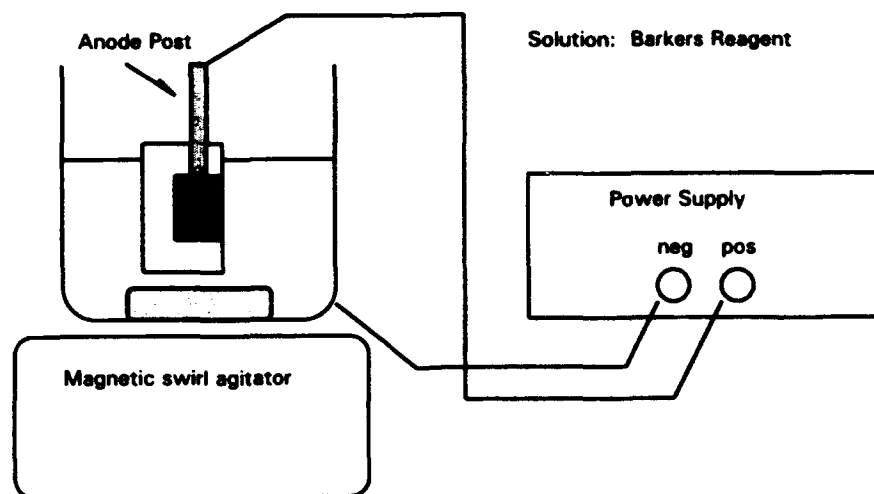


Figure 7. Anodizing configuration

IV. RESULTS AND DISCUSSION

A. PROCESSING RESULTS

1. Homogenization Heat Treatment

In a preliminary study, blistering was observed during homogenization treatments conducted at 560°C on MMC billets initially supplied. Subsequently it was found that matrix composition for this initial material was out of specification for 6061 and new materials were provided (designated as heats 1-1169 and 1-1095). Subsequent homogenization heat treatments were conducted for 20 hours at 530°C for both composite compositions and no further blistering was observed.

2. Forging

Initial hot working of all materials was accomplished by upset forging on heated platens immediately after completion of the homogenization treatment. Billets were transferred directly from the 530°C furnace. At first, sample billets were upset forged utilizing platen temperatures of 400°C and a press rate of 0.07 to 0.10 in/sec (1.7 to 2.5 mm/sec) corresponding to or a nominal strain rate of 0.03 sec⁻¹, such that upsetting was completed in 20 to 30 seconds. Relatively severe edge cracking associated with frictional constraint was observed for these conditions (Figure 8) [Ref. 28]. Increasing the platen temperatures to 480-500°C decreased the severity of the edge cracking and reduction of the strain rate to a nominal value of 0.020-0.025 sec⁻¹ eliminated nearly all surface indicators of edge cracking (Figure 9).

3. Rolling

Rolling was conducted with reheating between successive passes. In all cases the interpass annealing (IPA) temperature was 500°C. IPA times were either 5 or 30 minutes;

for a 5 minute IPA the furnace temperature fluctuated about 10°C during processing. Most of the billets were rolled without edge scarfing to remove the barreled regions from the lateral surfaces of the forgings. In several cases this resulted in severe edge cracking (Figure 10) which was later removed prior to machining tensile coupons. Alligatoring of the composite billets took place during rolling for thicknesses from 0.45 inches (12 mm) downward to 0.25 inches (6 mm). This cracking was limited in all cases to a region extending about 0.75 inches (18 mm) inward from the ends of the billets which were immediately re-rolled to close the cracking prior to being returned to the furnace for the IPA. Both edge cracking and alligatoring were more severe in the 20 vol. pct. MMC material. However, rolling with the 30 minute IPA resulted in less severe cracking for both particle volume fractions examined in this program.



Figure 8. As-forged billet of 6061 Al - 10 vol. pct. Al_2O_3 with severe longitudinal cracking for an upset forging rate of 0.07 to 0.10 in/sec.



Figure 9. As-forged billet of 6061 Al - 10 vol. pct. Al_2O_3 with only traces of longitudinal cracking following use of an upset forging rate of 0.02 to 0.025 in/sec.

The lateral surfaces of one billet were scarfed prior to rolling. In this case only minor edge cracking was experienced near the end of the rolling (Figure 11). The tendency to alligator was reduced as well. It is possible that industrial practices involving scarfing, use of edge rolls and mill rolls of larger diameters would significantly reduce the alligating problem encountered. Alligating is caused by stresses resulting from friction effects and sliding at the roll/workpiece interface as the material experiences longitudinal acceleration during the rolling pass. In all cases silicone spray was used to provide lubrication of the rolls. This was applied between rolling passes and prevented sticking of the MMC material to the roll surfaces.

The 3:1 reduction in height during upset forging corresponds to a true strain of about 1.1 while a true strain of 2.4 was imparted during rolling. Thus, the total strain during processing amounted to 3.5 for the composites (forging plus rolling). In contrast the strain added to the 6061-T6 plate during rolling was 2.4. The strain imparted during original manufacture of the 6061-T6 plate is unknown. No edge cracking or alligating was observed during processing of this unreinforced reference material.

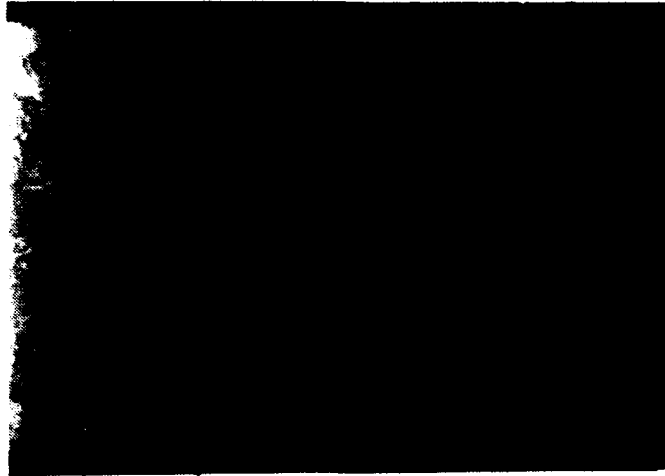


Figure 10. A rolled billet of 6061 Al - 10 vol. pct. Al_2O_3 exhibiting severe edge cracking. This billet had been scarfed prior to machining with approximately 36% wastage.

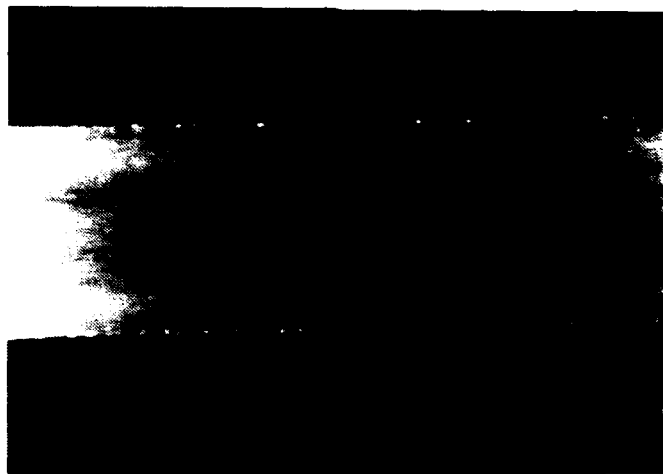


Figure 11. Rolled billet of 6061 Al - 10 vol. pct Al_2O_3 showing minor edge cracking. The billet had been scarfed prior to rolling (with ~30 % wastage) and prior to machining (with ~5 to 10% additional wastage).

4. Machining

Although diamond-impregnated bandsaw blades were utilized in sectioning of these materials prior to machining, extremely high blade wear rates were encountered. However, samples were satisfactorily milled using tooling with diamond inserts. The gage sections of the tensile test coupons were satisfactorily milled using a cobalt milling cutter. Coupons were gang machined in blocks of 15 yielding highly uniform tensile specimens.

With the 20 vol. pct. Al_2O_3 composite the cobalt cutters tended to burnish the material and smear the edges into the next coupon. This edge defect was removed by flat grinding prior to tension testing.

5. Tensile Testing

Tensile coupon design was deemed satisfactory. Fracturing occurred within the middle 2/3 of the gage section except for the 20 vol. pct. Al_2O_3 MMC following solution heat treatment at either 530 or 560°C. For these process conditions the material was very sensitive to stress concentration at the extensometer knife edges (Figure 12). In these cases the coupons failed prior to attaining an ultimate tensile strength.

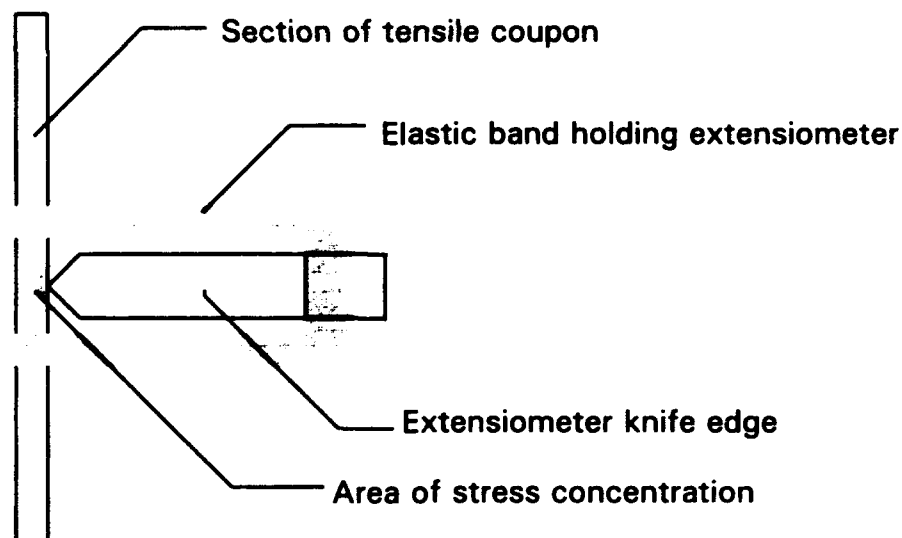


Figure 12. Schematic detail of extensometer contact point with the tensile coupon illustrating the stress concentration point.

B. OPTICAL MICROSCOPY RESULTS

1. The Unreinforced 6061 Material

a. The as-received condition

The as-received 6061 was in the form of a plate 26 mm in thickness obtained from stock available at NPS. The microstructure of this material (Figure 13) is typical of rolled aluminum alloys and exhibits highly elongated grains. Mechanical fibering of inclusions is reflected in their alignment with the rolling direction. From the as-received condition this material was subjected to the same procedures employed for the MMCs and thus provides a basis of comparison of the data obtained on the composites.

b. The as-rolled condition

Rolling of the unreinforced 6061 material was conducted at 500°C with either 5 or 30 minute IPA times, just as for the composites. In the as-rolled condition the grains were further flattened and extended in comparison to the as-received material although some of the grains appear shortened, suggesting that some grains may be pinched off during this additional processing. There is little difference in the as-rolled microstructure attributable to the different interpass anneal times. (Figure 14).



Figure 13. As-received 6061 Al-T6 plate, illustrating the elongated grain structure (grains $\approx 1\text{mm}$ in length). The structure also shows inclusions aligned with the rolling direction.



Figure 14. The as-received 6061 material illustrating the microstructure after the final rolling pass (true strain of 2.4).

c. Solution heat treated condition.

The effect of subsequent solution treatment on the unreinforced 6061 material is shown in Figure 15. Grains have coarsened and now appear to be less highly elongated than in either the as-received or the as-rolled conditions. The IPA time during prior rolling again did not appear to have had a discernible effect on the grain size following subsequent solution heat treatment. Also, there was relatively little effect of the solution treatment temperature on the microstructure.



Figure 15. The rolled and solution heat treated 6061 (5 minutes IPA time) illustrating the microstructure after solution treatment 480°C for 1 hr.

2. 6061 Al - 10 Vol. Pct. Al_2O_3

The influence of forging and subsequent rolling on the distribution of the Al_2O_3 particles was assessed metallographically on unetched samples examined with conventional light microscopy methods. The matrix microstructure was examined using polarized light techniques in conjunction with anodized samples. These methods allowed

evaluation of MMC processing parameters on both the reinforcement particle distribution and the matrix microstructure.

a. Particle redistribution during processing

The particle distribution in the as-cast material was highly non-uniform as can be seen in Figure 16. This likely is due to segregation of particles into interdendritic regions during solidification. The particle distribution in this as-cast material appears somewhat more uniform than that reported by Schaefer [Ref. 13] on an older heat representing an earlier version of this same MMC composition. This suggests that improvements have been made in the casting process for these MMC materials. Close inspection of the micrograph of Figure 16 also reveals the presence of relatively fine Mg_2Si second phase particles.

The uniformity of the Al_2O_3 distribution was improved by the forging operation, which involved a true strain of about 1.0, but the particles are not yet homogeneously distributed (Figure 17). Instead, the clusters have changed in shape, reflecting the forging strain, and particles within the clusters now appear to be more widely separated. These clusters will result in banding upon subsequent rolling.

In this work, the particle distribution was examined again after the completion of the final rolling pass. At that point, the total processing strain (forging + rolling) was 3.5 and the particle distribution appears to be nearly uniform and homogeneous as shown in Figure 18. Some banding is evident and particles are aligned in the rolling direction. In a closely related study, Longenecker [Ref. 21] has considered this redistribution of particles during processing in greater detail and has compared observed and computer-simulated particle distributions. It was noted that there is no quantitative measure of uniformity or homogeneity for such distributions but that a processing strain ≈ 5.0 resulted in observed distributions which were indistinguishable from simulated random distributions.

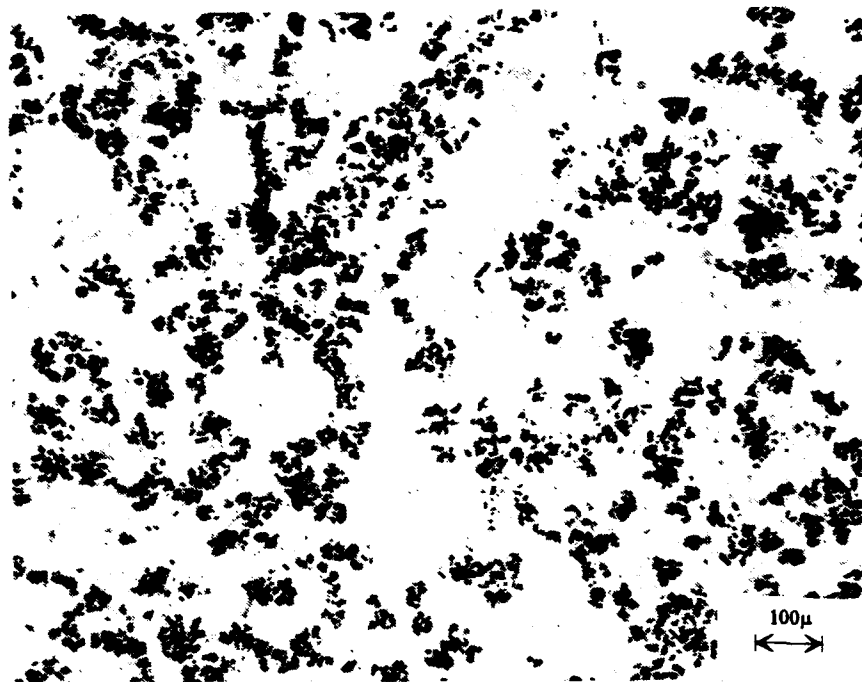


Figure 16. A micrograph of the as-cast 6061 Al - 10 vol. pct. Al₂O₃ composite illustrating the inhomogeneity of the particle distribution. Polished (not etched).



Figure 17. The forged 6061 - 10 vol. pct. Al₂O₃ MMC illustrating redistribution of the particles during straining. Polished (not etched).



Figure 18. The as-rolled 6061 Al - 10 vol. pct. Al₂O₃ composite illustrating further redistribution of the particles during rolling. Polished (not etched).

b. Effect of processing on the matrix microstructure

The matrix of this MMC in the as-cast condition displays large, irregular grains of 0.25 - 0.30 mm (250 - 300 μm) diameter. Relatively fine Mg₂Si precipitates are evident and close examination indicated the presence of inclusions which were judged to be Fe or Si phases formed during casting shown (Figure 19). A coarse grain size such as this has been suggested to confer low matrix strength [Ref. 18, 22] in the composite. Homogenization to facilitate hot working was accomplished by heating for 20 hours at 530°C and the result of the treatment is shown in Figure 20. Resolutioning of the Mg₂Si is apparent; the homogenization treatment had no effect on either the particle distribution or the matrix grain size.

The grain shape change during forging is similar to the redistribution of particles occurring during this process. Unrecrystallized grains have become flattened

(Figure 21) while partial recrystallization has resulted in the formation of some grains near the size predicted by PSN (Figure 1). The unrecrystallized grains appear to be about 20 μ m in thickness. Approximately 5-10% of the grain structure appears to be recrystallized to sizes varying from \approx 5 μ m to \approx 30 μ m, reflecting the non-uniform particle distribution.

After the final rolling pass, a refined but distorted grain structure is developed as shown in Figure 22. A similar fine-grain structure was observed for both IPA times and grain sizes of about 18 μ m were measured in each case. Such a structure likely reflects successive PSN of recrystallization during the reheating intervals between latter passes of the rolling schedule and the distortion due to the rolling deformation is retained immediately following completion of the final pass. The effect of reheating the as-rolled material (either IPA time during prior rolling) for five minutes at 500°C is shown in Figure 23. The deformed grains present after the final rolling pass have been replaced by fine, equiaxed grains and the structure appears to be completely recrystallized. PSN of recrystallization has been shown [Ref. 9] to occur with a five-minute IPA during processing of this material at 350°C and the deformation parameters met the conditions for PSN given by Humphreys [Ref. 17] for the 12 μ m particles in this MMC. Little further change in the matrix grain structure is seen upon heating of this material for one hour at 560°C for solution treatment (Figure 24). It is noteworthy that many grains appear to have six sides, indicating a narrow grain size distribution and a uniform, equiaxed structure. Neither the solution treatment temperature nor the IPA time during prior rolling had any apparent effect on the recrystallized grain size following solution heat treatment. It appears that PSN is the controlling mechanism and this corresponds to site saturation during recrystallization. Thus grain growth will be limited once new grains impinge and this is reflected by the large number of six-sided grains.

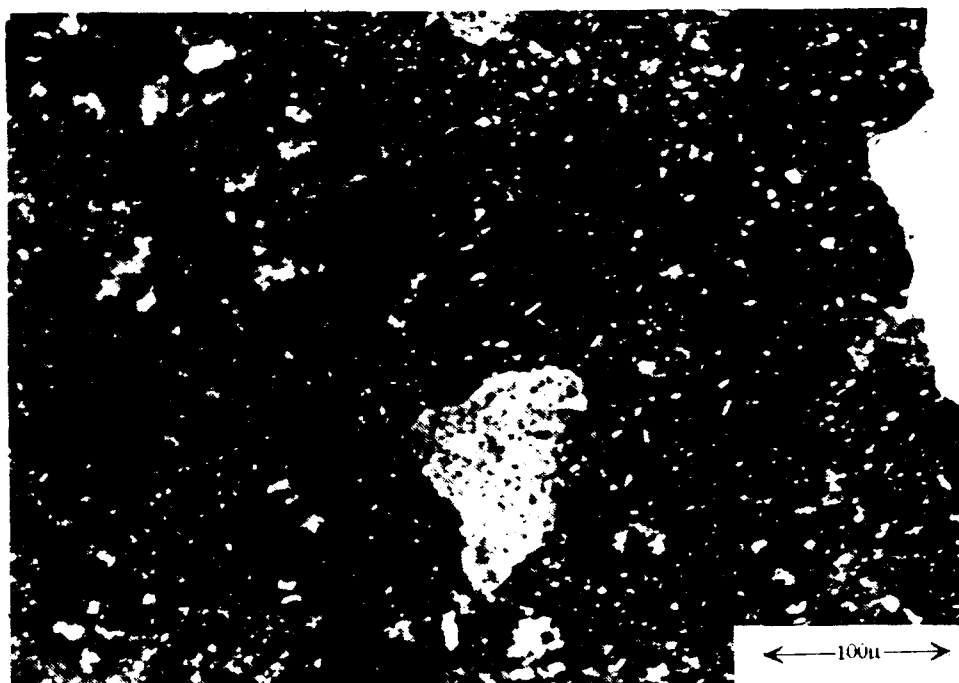


Figure 19. The as-cast 6061 Al- 10 vol. pct. Al_2O_3 composite illustrating a coarse and irregular grain structure.

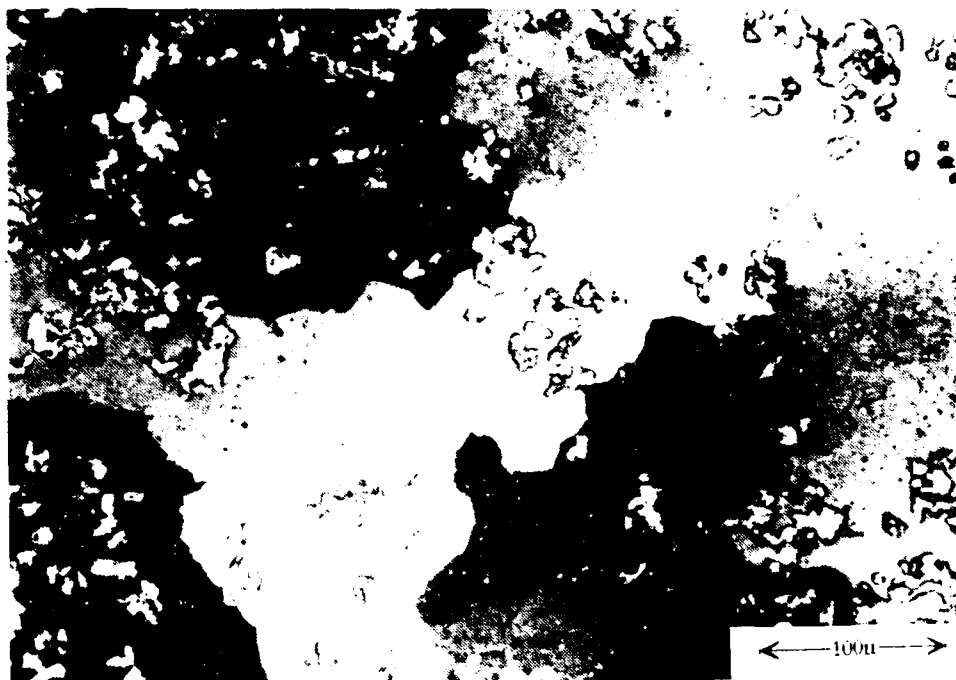


Figure 20. As-cast and homogenized 6061 Al - 10 vol. pct. Al_2O_3 composite illustrating the same grain structure and the resolution of the Mg_2Si .

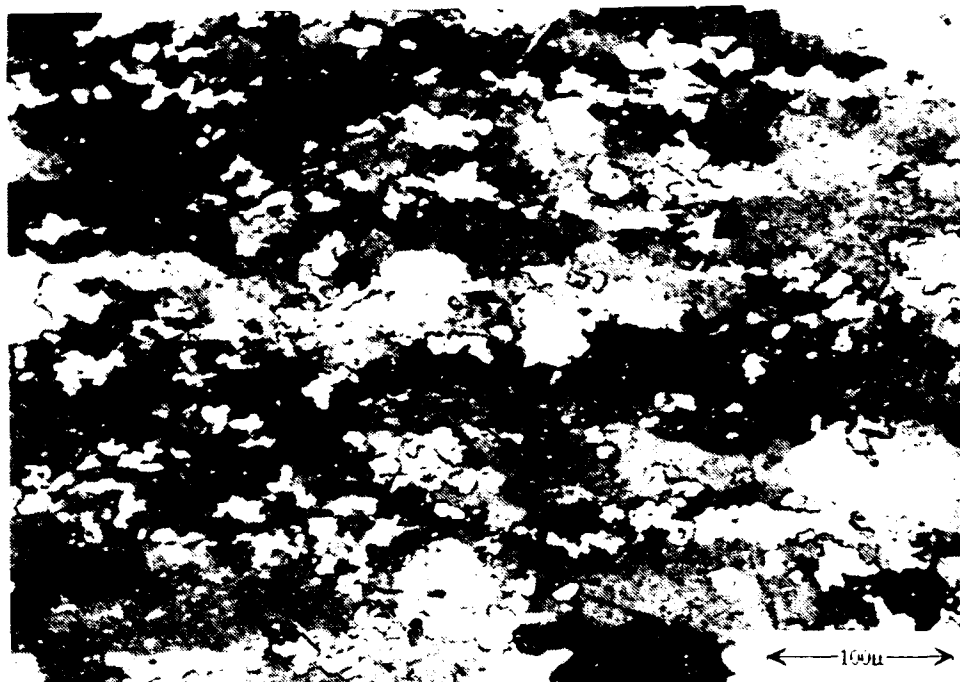


Figure 21. The forged 6061 Al- 10 vol. pct. Al₂O₃ MMC, illustrating grain refinement of the matrix.

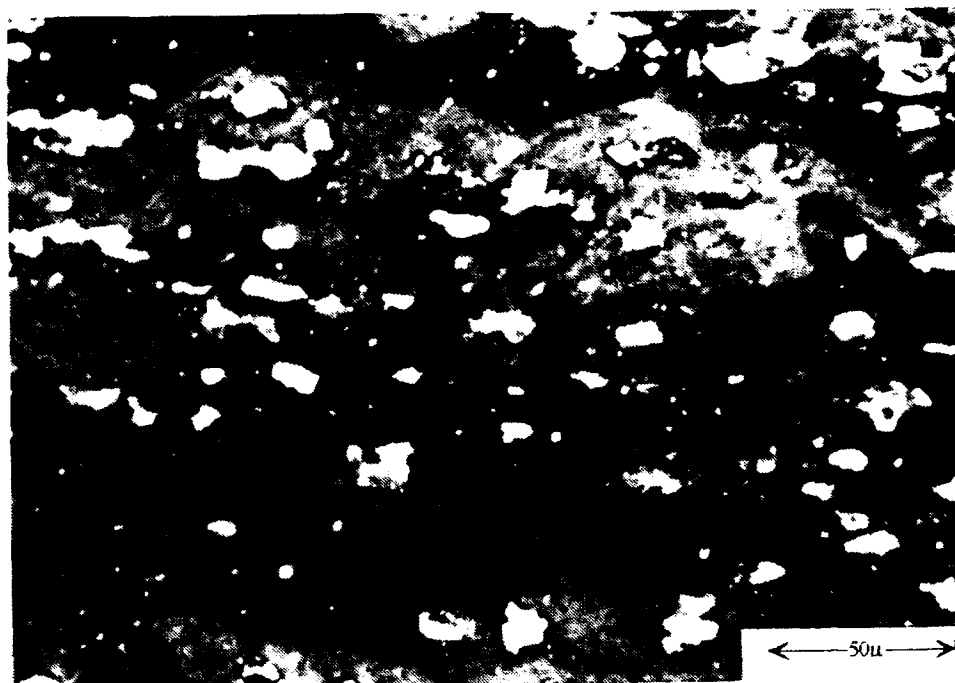


Figure 22. The as-rolled condition for the 6061 Al - 10 vol. pct. Al₂O₃ material illustrating distortion by rolling deformation of a previously recrystallized grain structure.

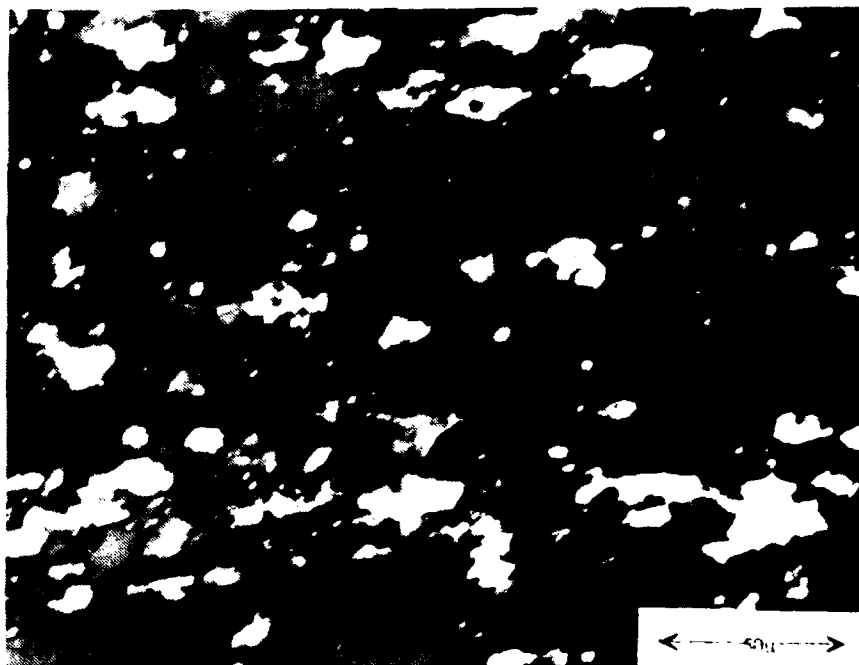


Figure 23. Reheating of the rolled 6061 Al - 10 vol. pct. Al_2O_3 material for 5 minutes at 500°C results in PSN of recrystallization.

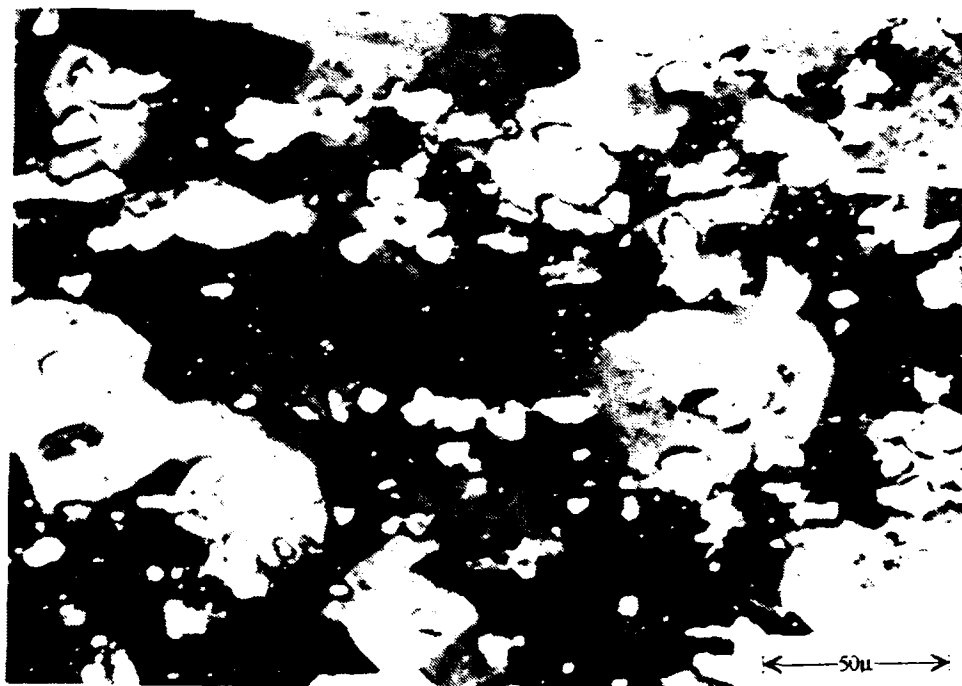


Figure 24. The effect of solution heat treatment for one hour at 560°C on the rolled 6061 Al - 10 vol. pct. Al_2O_3 composite, showing PSN of recrystallization. The particle spacing appears to be the controlling factor in grain size.

3. 6061 Al - 10 Vol. Pct. Al_2O_3

a. The particle distribution

The Al_2O_3 particles in this as-cast MMC material appear to be more uniformly distributed in comparison to the particles in the lower volume fraction composite. This may be seen by comparing Figure 25 (20 vol. pct.) to Figure 16 (10 vol. pct.). The larger particles are apparently less affected by growing dendrites during solidification and thus are less segregated in the as-cast condition. The only other features noted were the relatively fine precipitates of the Mg_2Si phase. The forging process has resulted in some particle redistribution and a nearly homogeneous structure is achieved at this point in the processing as shown in Figure 26.

The forging and rolling processes employed with this 20 vol. pct. MMC were identical to those used with the lower volume fraction material. At the completion of the final rolling pass (total forging + rolling strain of 3.5) some further homogenization of the particle distribution is seen (Figure 27). Many of the finer particles in this material are elongated, with an aspect ratio of 2-3 and these have become oriented with their long dimension parallel to the rolling direction.

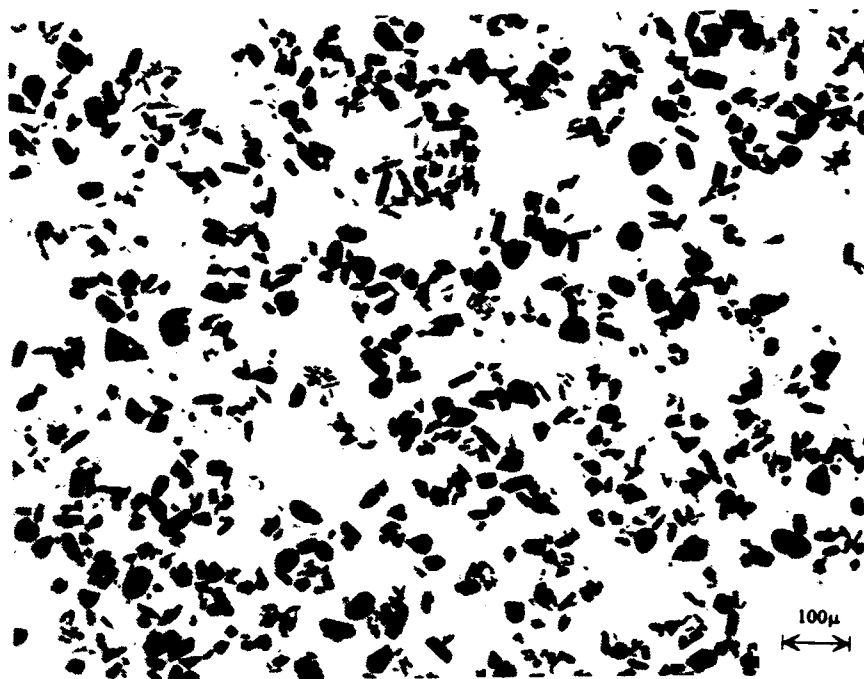


Figure 25. The particle distribution in the as-cast 6061 Al - 20 vol. pct. Al₂O₃ composite illustrating greater homogeneity than apparent in the 10 vol. pct. Al₂O₃ material (see Figure 16). As polished (not etched).

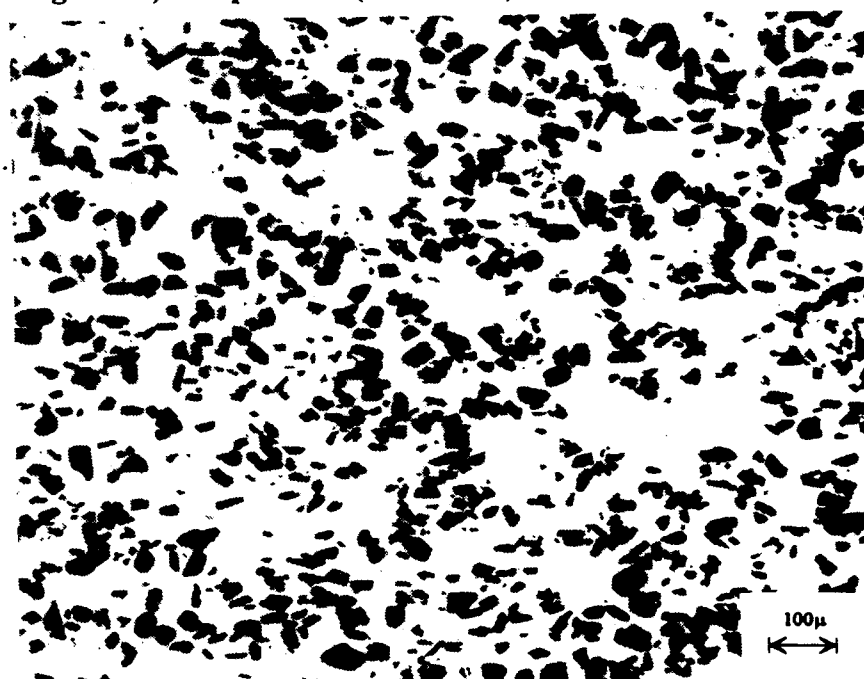


Figure 26. The forged 6061 Al - 20 vol. pct. Al₂O₃ MMC, illustrating improved homogeneity of the particle distribution. As-polished (not etched).

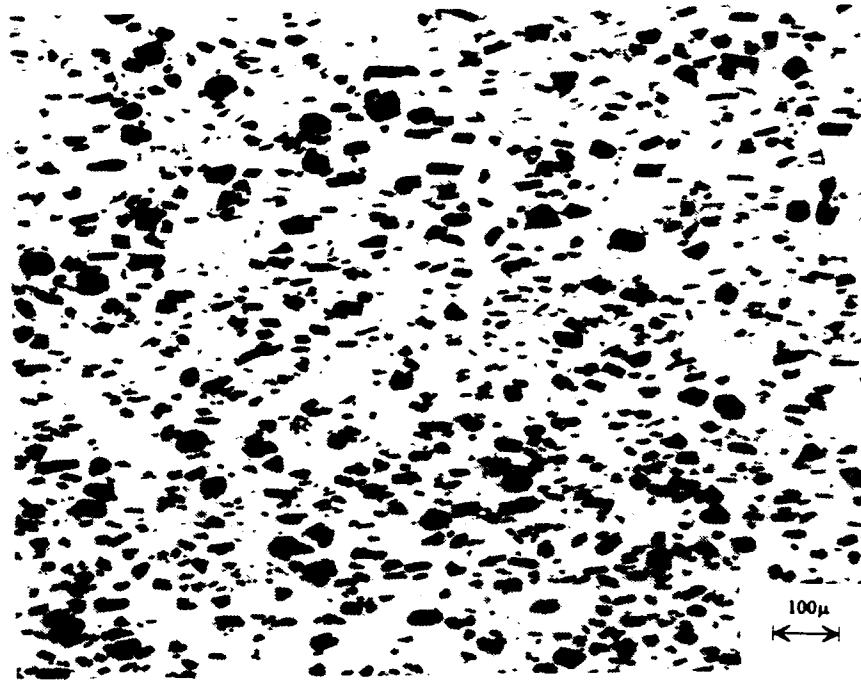


Figure 27. The rolled 6061 Al - 20 vol. pct. Al₂O₃ material showing an essentially homogeneous particle distribution but with the alignment of particles in the rolling direction. As polished (not etched).

b. Effect of processing on matrix microstructure in the 20 vol. pct. Al₂O₃ MMC.

In the as-cast condition the matrix of this MMC displays a coarse, irregular structure with a grain diameter of about 0.25 to 0.30 mm (250 - 300μ) when the sample is anodized and viewed under crossed polars. Numerous, fine particles of Mg₂Si as well as Fe and Si containing precipitates formed during casting are also apparent as shown in Figure 28.

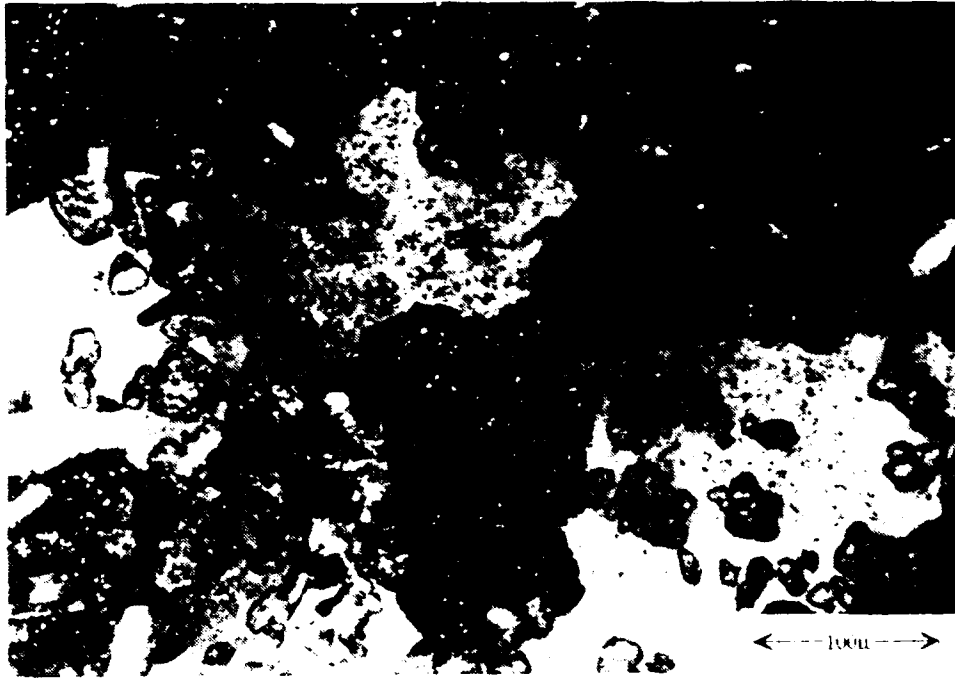


Figure 28. The as-cast 6061 Al - 20 vol. pct. Al₂O₃ composite showing coarse, irregular grains. Anodized and examined under crossed polars.

The homogenization treatment (530°C for 20 hrs.) caused resolutioning of the soluble phases, in particular the Mg₂Si. There was no apparent evidence of recrystallization in the matrix due to the homogenization and a coarse and irregular grain structure similar to that in the as-cast material was seen (Figure 29).

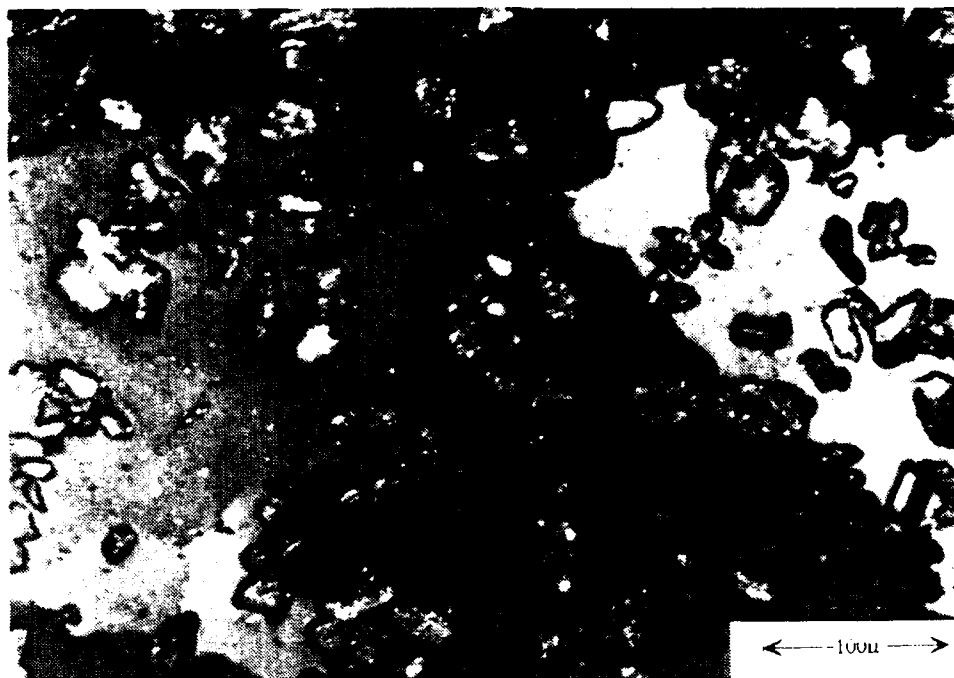


Figure 29. The as-cast and homogenized 6061 Al - 20 vol. pct. Al₂O₃ composite illustrating the same coarse and irregular grain structure as in the as-cast condition. Anodized and examined under crossed polars.

Following the forging operation, a completely recrystallized grain structure was observed in this 20 vol. pct. Al₂O₃ material (Figure 30). The grain size corresponds reasonably well to the value dictated by the PSN theory for particles of the size present in this MMC and the largest observable grains are about 40 μm in size.

The grain structure immediately following the final rolling pass is shown in Figure 31. In spite of the quenching effect of the rolls and rapid cooling of the relatively thin as-rolled sheet, recrystallization has begun and some regions appear to be fully recrystallized. Thus recrystallization due to PSN is rapid. Grain size values were the same for both 5 and 30 minute IPA times indicating again that there is little grain growth upon completion of recrystallization. For material rolled with the 5 minute IPA a coupon was reheated for 5 minutes, at 500°C and the matrix microstructure was then examined. It is fully recrystallized, as shown in Figure 32, and the grain size is essentially the same as seen in the as-rolled material (Figure 31).

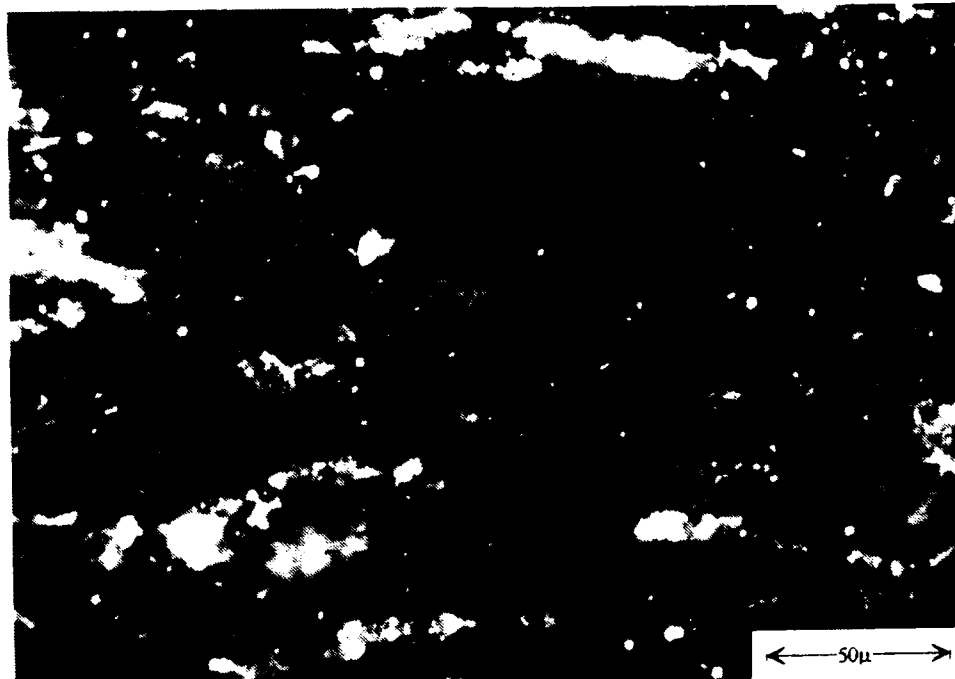


Figure 30. As-Forged 6061 Al - 20 vol. pct Al_2O_3 composite illustrating PSN of recrystallization in the grain structure on completion of forging.

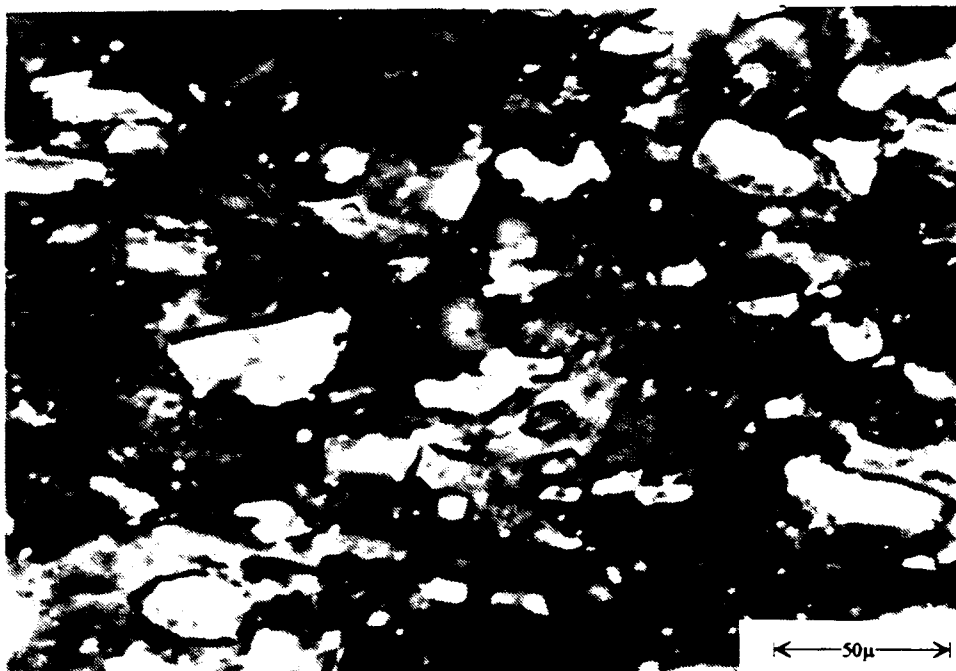


Figure 31. As-rolled 6061 Al - 20 vol. pct. Al_2O_3 composite illustrating deformation by rolling of the previously recrystallized grain structure.

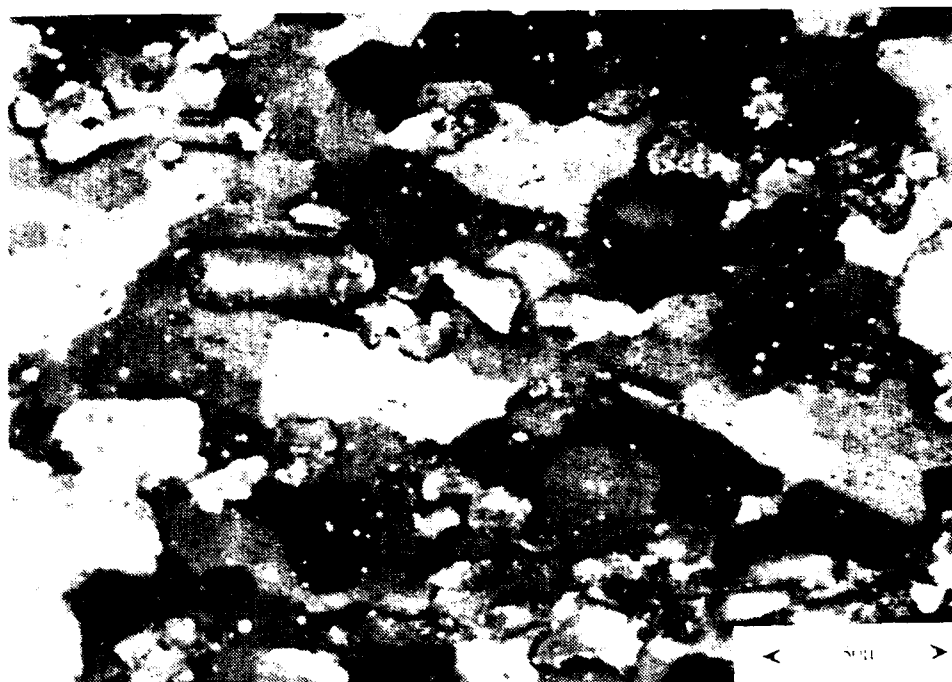


Figure 32. Rolled 6061 Al - 20 vol. pct. Al_2O_3 composite illustrating complete PSN of recrystallization after reheating of a coupon for 5 min. at 500°C .

There is little further change in microstructure following solution heat treatment. The matrix grain structure is shown in Figure 33 for material which has been rolled with a 30 minute IPA and then solution heat treated for one hour at 560°C . Comparison of this structure to those shown in Figures 30 and 32 reveals little significant difference. Examination of microstructures following solution heat treatment at various temperatures showed that neither the solution treatment temperature nor the IPA time affected the recrystallized grain size. It again appears that PSN is the controlling mechanism in the recrystallization and that growth occurs only until the newly formed grains impinge on another one. If essentially all particles are nucleation sites then the grain size will be given by the particle spacing. It is again noteworthy that the recrystallized grains are equiaxed and often six sided. This is consistent with simultaneous nucleation of the grains at uniformly distributed sites which results in turn in a uniform, narrowly distributed grain size in the material.



Figure 33. The microstructure of a rolled and solution heat treated 6061 - 20 vol. pct. Al_2O_3 composite illustrating complete recrystallization via PSN. Solution heat treatment was for one hour at 560°C . Anodized and viewed under crossed polars.

C. HEAT TREATMENT AND MECHANICAL PROPERTIES

1. Unreinforced 6061

The effect of processing parameters on subsequent heat treatment response of the unreinforced 6061 alloy was evaluated to provide a basis for comparison to corresponding composite data. Solution heat treatment temperatures varied from 480 - 560°C; subsequent aging was always accomplished at 160°C. The data for unreinforced 6061 revealed no dependence on the IPA time of the prior TMP schedule and this is consistent with the similarity of microstructures for the material when processed with either of these IPA times. Figures 34 - 37 present ductility, yield strength, tensile strength and hardness data for aging following rolling with the 30 min. IPA time and these data are representative of that for the material processed with the 5 min. IPA. Data in graphical form for the 5 minute IPA are presented in Appendix C for ductility, yield strength, ultimate strength and hardness. In all cases, the data plotted for one minute aging time correspond to the solution treated condition.

The ductility of this unreinforced 6061 material depends only weakly on solution heat treatment temperature. On the other hand, use of higher solution heat treatment temperatures substantially improves the subsequent aging response and raises the peak strength and hardness of this material. This likely reflects an increased solute content in the solid solution upon solution treatment at higher temperatures and therefore the attainment of a greater precipitate volume fraction during subsequent aging. The data obtained here for solution heat treatment at temperatures 530 - 560°C is identical to Handbook data [Ref. 29] for the same heat treatment conditions. A peak yield strength of 275 MPa occurred at 13.3 hrs. of aging at 160°C following solution heat treatment at 530°C in the data of this work and these data are identical to Handbook [Ref. 29] values for this alloy.

6061 Al 30 min IPA at 500C

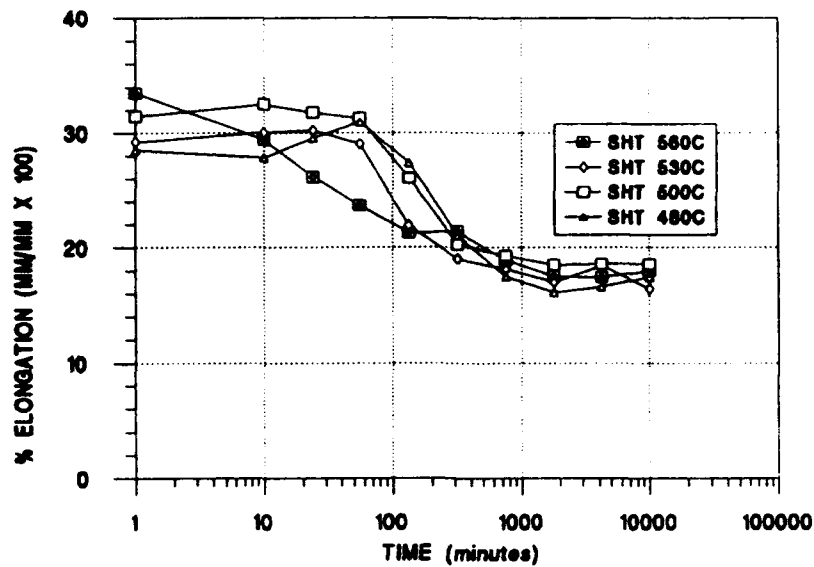


Figure 34. Plot of elongation versus aging time for unreinforced 6061 material processed utilizing a 30 min. IPA during rolling at 500°C. Data are included for four different solution heat treatment temperatures.

6061 Aluminum 30 min IPA at 500C

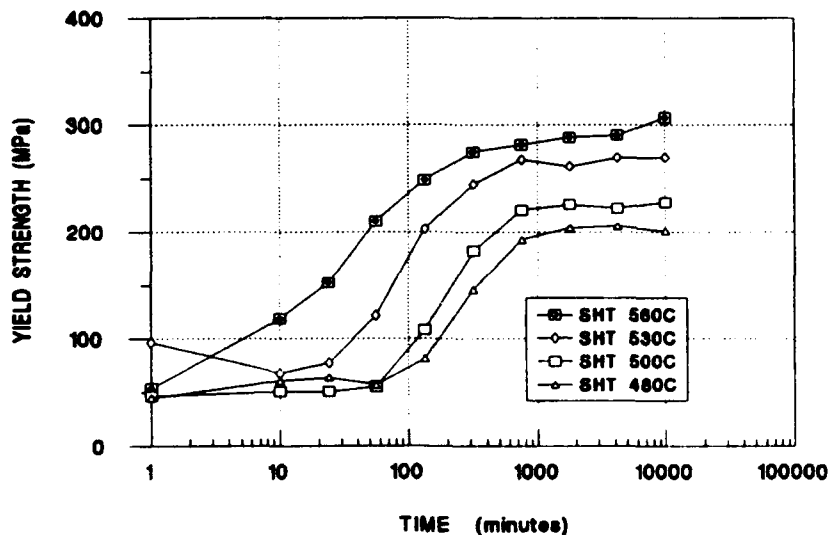


Figure 35. Plot of yield strength versus aging time for unreinforced 6061 material processed utilizing a 30 min. IPA during rolling at 500°C. Data are included for four different solution heat treatment temperatures.

6061 Al - 30 min IPA at 500C

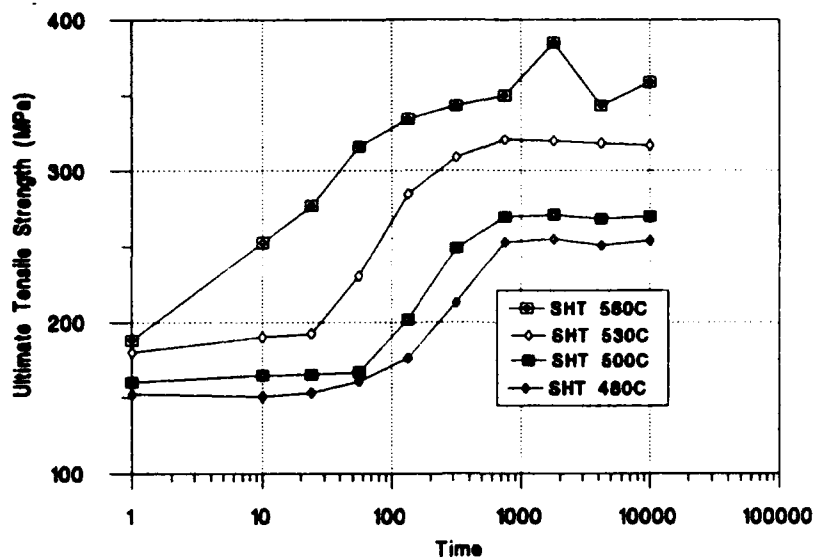


Figure 36. Plot of ultimate tensile strength versus aging time for unreinforced 6061 material processed utilizing a 30 min. IPA during rolling at 500°C. Data are included for four different solution heat treatment temperatures.

6061 Aluminum 30 min IPA at 500C

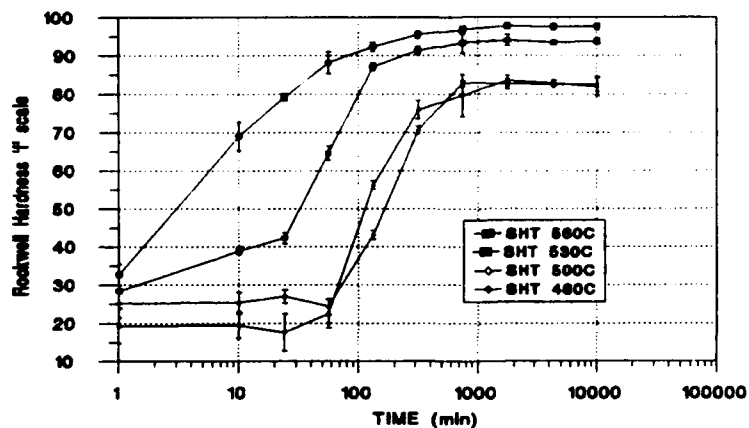


Figure 37. Plot of hardness versus aging time for unreinforced 6061 material processed utilizing a 30 min. IPA during rolling at 500°C. Data are included for four different solution heat treatment temperatures.

2. The 6061 - 10 Vol. Pct. Al_2O_3 MMC

Figures 38 - 41 illustrate the mechanical property data obtained following heat treatment of the 10 vol. pct. material. No dependence on the IPA time during rolling was noted, except for lower solution heat treatment temperatures. Then, a small improvement in ductility was found for the 30 minute IPA material. Only the data for material processed with the 30 minute IPA time will be presented in this section: data for the 5 minute IPA material is summarized in the Appendix. (Appendix C provides graphical presentations of the tabular data in Appendix B for the 5 minute IPA material.)

The most notable difference between the aging response of the composite and that of the unreinforced 6061 is an increase in the ductility associated with the use of lower solution heat treatment temperatures. The ductility obtained for the peak-aged condition following solution treatment at 480°C was about 10% elongation to failure. In contrast, lower ductilities of 6 - 8 % elongation accompanied solution heat treatment at higher temperatures of $530 - 560^\circ\text{C}$. The yield and ultimate strength and the hardness data all exhibited the same trends as seen in the data for the unreinforced material in that increased solution treatment temperature resulted in improved aging response. Comparison of the data in Figures 34 - 37 with those in Figures 38 - 41 reveals that the composite is always stronger but less ductile for otherwise identical processing and heat treating conditions. Thus, the addition of particles results in strengthening of the material as well as an increased modulus of elasticity. Values of Young's modulus, E , were determined by measuring the slopes of the elastic portions for the stress-strain curves obtained in this study. The average value for this 10 vol. pct. material was 85 ± 5 GPa.

Significantly higher ductilities were reported for heat treated material in previous research on additional TMP by rolling of an initially extruded 6061 Al - 10 vol. pct. Al_2O_3 MMC [Ref. 17] . The total strain achieved in processing of the MMC was > 5.0 in

Eastwood's work [Ref. 17] while that attained by the forging and rolling of this research was about 3.5. In a parallel study by Longenecker [Ref. 21], particle redistribution during processing of this 10 vol. pct. MMC material was examined metallographically. Processing methods included the rolling of this study as well as combinations of extrusion operations involving strains up to ≈ 5.3 [Ref. 17]. Improving homogeneity of the particle distribution was noted by Longenecker [Ref. 21] for strains exceeding 3.5 and on up to the largest value attained. Thus, it appears that the tensile ductility of this material is quite sensitive to the particle distribution. Also, improvements in distribution achieved through process control, including solidification as well as deformation processes, will likely result in better ductility in the final product.

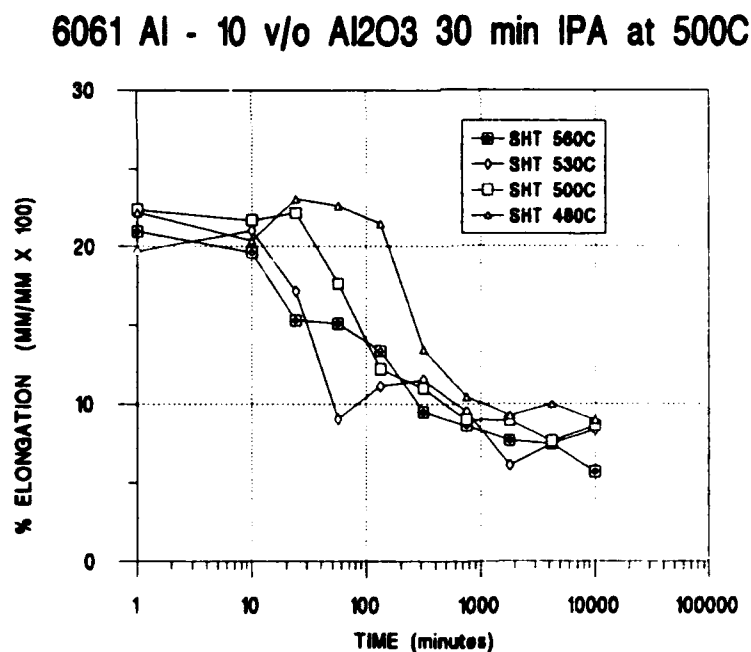


Figure 38 . Plot of elongation versus aging time for 6061 Al - 10 vol. pct. Al₂O₃ material processed utilizing a 30 min. IPA during rolling at 500°C. Data are included for four different solution heat treatment temperatures.

6061 Al - 10 v/o Al₂O₃ 30 min IPA at 500C

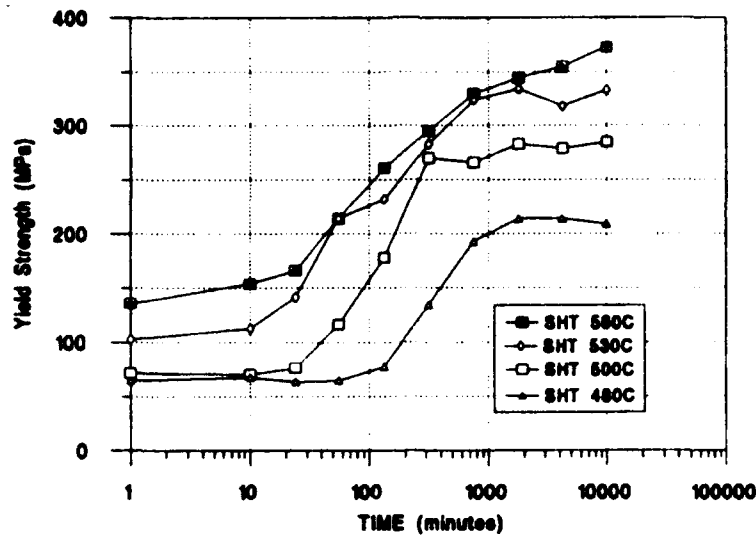


Figure 39. Plot of yield strength versus aging time for 6061 Al - 10 vol. pct. Al₂O₃ material processed utilizing a 30 min. IPA during rolling at 500°C. Data are included for four different solution heat treatment temperatures.

6061 Al -10 v/o Al₂O₃ 30 min IPA at 500C

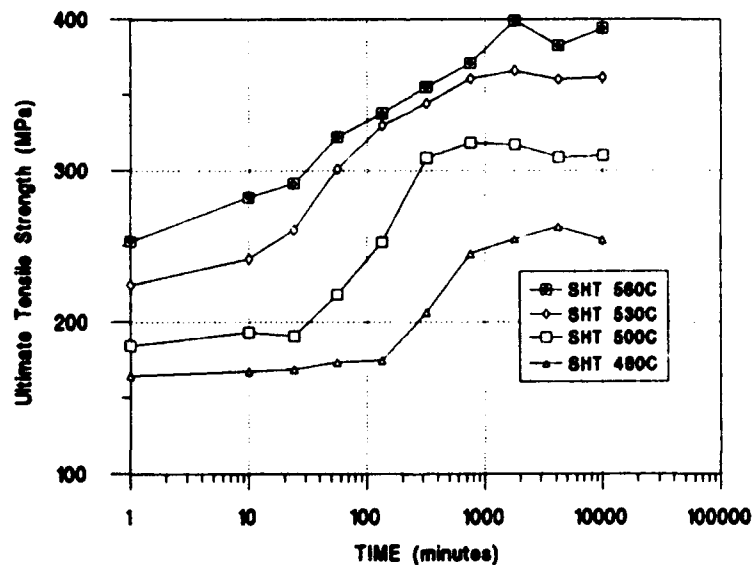


Figure 40. Plot of ultimate tensile strength versus aging time for 6061 Al - 10 vol. pct. Al₂O₃ material processed utilizing a 30 min. IPA during rolling at 500°C. Data are included for four different solution heat treatment temperatures.

6061 Al - 10 v/o Al₂O₃ 30 min IPA at 500C

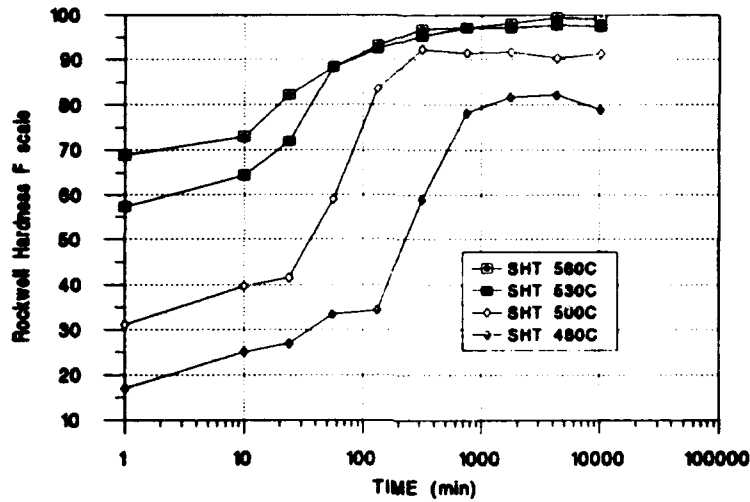


Figure 41. Plot of hardness versus aging time for 6061 Al - 10 vol. pct. Al₂O₃ material processed utilizing a 30 min. IPA during rolling at 500°C. Data are included for four different solution heat treatment temperatures.

3. 6061 Al - 20 Vol. Pct. Al₂O₃

A similar series of heat treatments were conducted on the 6061 Al - 20 vol. pct. Al₂O₃ MMC following completion of processing. Comparison of data for the two IPA times utilized in the prior TMP again reveals a small improvement in ductility for material processed with the 30 minute IPA time especially with lower solution heat treatment temperatures. Figures 42 - 45 illustrate the mechanical test results for the material processed with the 30 minute IPA as well. Data for the 5 minute IPA are included in the Appendix. The 20 vol. pct. material is generally stronger but lower in ductility when compared to the unreinforced and 10 vol. pct. materials.

The ductility of the 20 vol. pct. composite is improved by use of a lower solution heat treatment temperature in a manner similar to that of the 10 vol. pct material. However, the ductility is typically only about one-half that of the lower volume fraction composite even though both yield and ultimate tensile strengths are similar for the same processing and heat

treating schedules. The coarser particles present in the 20 vol. pct. composite might fracture more readily and thus account for at least some ductility reduction. Microstructural assessment of these materials following deformation to fracture was beyond the scope of this work. The Young's modulus was computed as for the lower volume fraction material and an average value of 92 ± 4 GPa was obtained.

6061 Al - 20 v/o Al_2O_3 30 min IPA at 500C

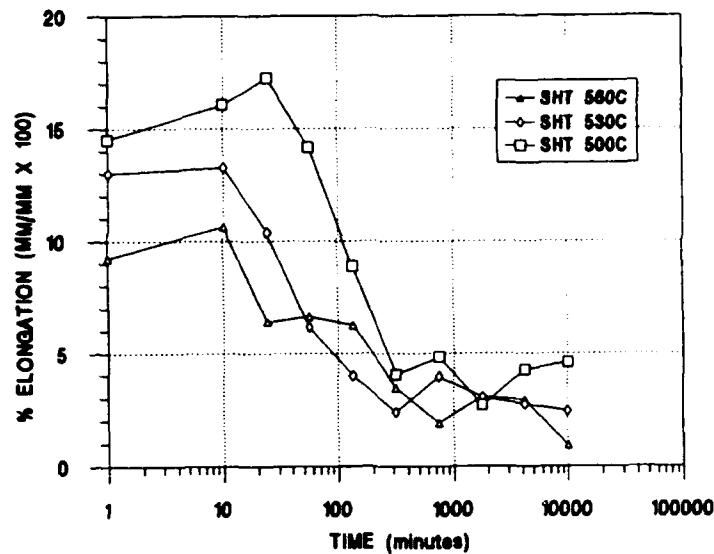


Figure 42. Plot of elongation versus aging time for 6061 Al - 20 vol. pct. Al_2O_3 material processed utilizing a 30 min. IPA during rolling at 500°C. Data are included for three different solution heat treatment temperatures.

6061 Al - 20 v/o Al₂O₃ 30 min IPA at 500C

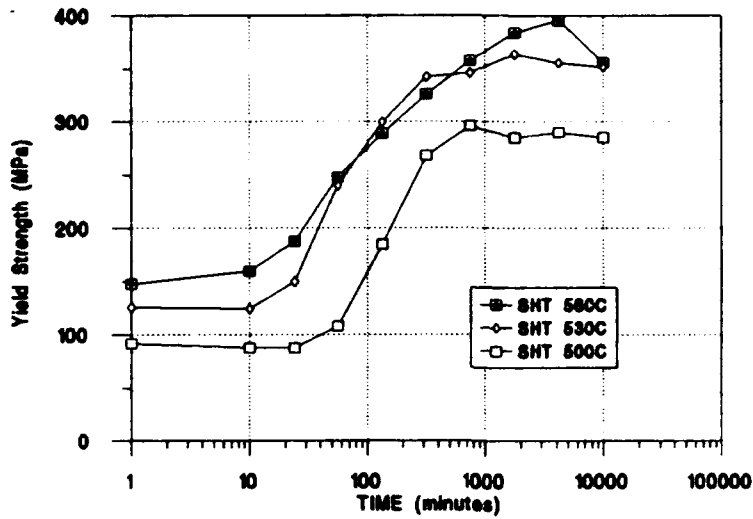


Figure 43. Plot of yield strength versus aging time for 6061 Al - 20 vol. pct. Al₂O₃ material processed utilizing a 30 min. IPA during rolling at 500°C. Data are included for three different solution heat treatment temperatures.

6061 Al - 20 v/o Al₂O₃ 30 min IPA at 500C

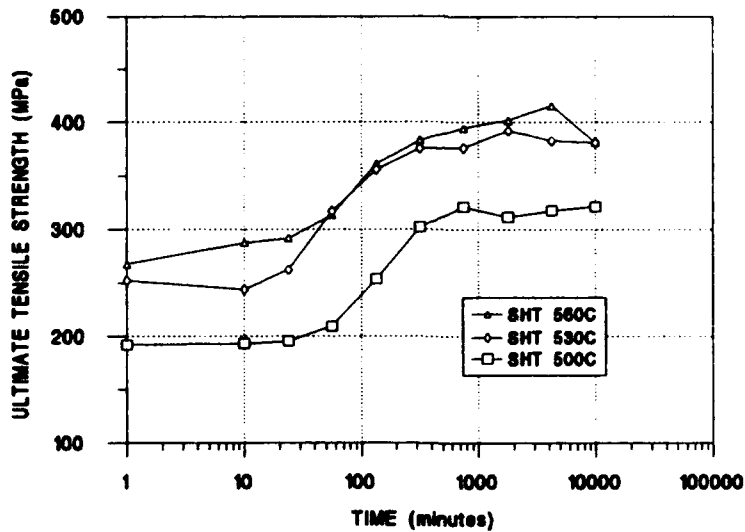


Figure 44. Plot of ultimate tensile strength versus aging time for 6061 Al - 20 vol. pct. Al₂O₃ material processed utilizing a 30 min. IPA during rolling at 500°C. Data are included for three different solution heat treatment temperatures.

6061 Al - 20 v/o 30 minute IPA at 500C

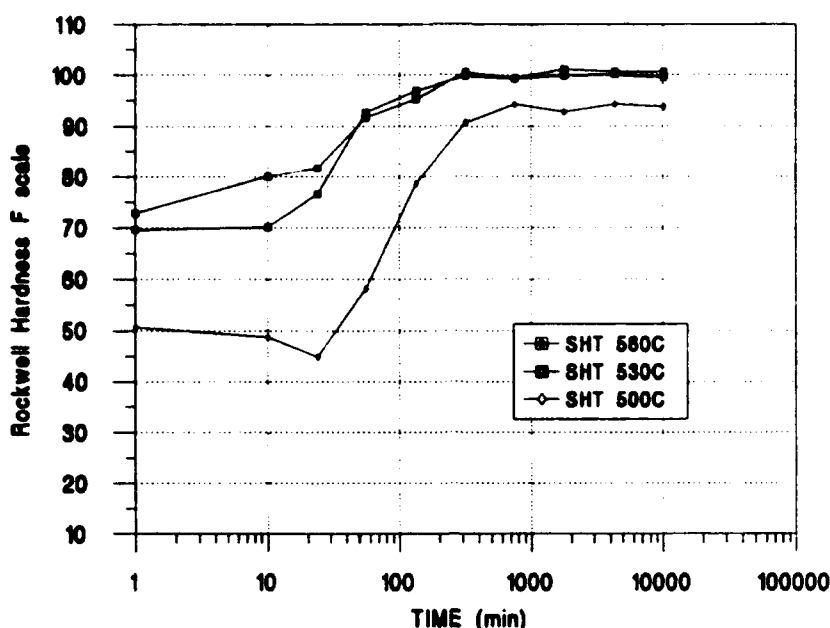


Figure 45. Plot of hardness versus aging time for 6061 Al - 20 vol. pct. Al_2O_3 composite material processed utilizing a 30 min. IPA during rolling at 500°C. Data are included for three different solution heat treatment temperatures.

4. Ductility Considerations

Examination of the mechanical property data for the 10 vol. pct. MMC material reveals that ductility enhancement can be accomplished by use of reduced solution heat treatment temperatures in combination with short aging times. Thus, elongations of 10% can be obtained with the 6061 Al - 10 vol. pct. Al_2O_3 MMC by use of solution temperatures of 480 - 500°C in combination with short aging times of 10 - 13 hours. Corresponding yield strengths up to 270 MPa could be attained with this material for a solution heat treatment of 500°C. Comparison of these results with the previous work by Eastwood [Ref. 17] demonstrates the importance of strain during processing and the control of the reinforcement particle distribution. Higher ductilities of 10-14% elongation were reported [Ref. 17] for a processed and heat treated 10 vol. pct. Al_2O_3 composite

containing 12 μ m particles. The essential difference in processing and heat treating appears to be the total strain achieved in the TMP prior to heat treatment. The material evaluated by Eastwood [Ref. 17] had been subjected to a total strain of 5.8 while the material of the current effort have experienced a strain of 3.5

The data of this research also indicates that 10% elongation is not attainable in the 20 vol. pct. material in heat treated material. Again, reduced solution heat treatment at lower temperatures appears to offer some ductility benefit but overall ductility is likely to be lower for this composite composition.

V. SUMMARY

A. CONCLUSIONS

The following conclusions are drawn from this work.

1. As-cast material can be processed by forging and rolling for suitable combinations of process parameters.
2. The TMP resulted in redistribution of the reinforcement particles due to the straining during processing.
3. Matrix grain refinement was achieved by PSN of recrystallization during processing.
4. The grain size of fully processed material can be estimated based on the PSN theory.
5. The TMP developed for the MMCs has little effect on the properties of unreinforced 6061 Al.
6. Enhanced ductility can be achieved for the MMC by processing to sufficient strain and by selecting appropriate heat treatment conditions, especially the solution heat treating temperatures.

B. RECOMMENDATIONS FOR FURTHER STUDY

1. Further characterization of microstructure is necessary to quantify effect of processing on particle distribution and on matrix grain structure. Methods should include pole figure determination by X-ray diffraction as a further means to assess recrystallization mechanisms.
2. Assess recrystallization during selected interpass anneals to determine the minimum time necessary to achieve a fully recrystallized condition.
3. Investigate the relationship between ductility and aging time to determine factors responsible for improved ductility in underaged samples.
4. Conduct particle size analysis to determine if there is significant particle fracturing during processing.
5. Investigate overaging behavior of these materials to determine if the ductility may be regained.
6. Investigate particle size analysis of the 20 vol. pct. composite to determine if particle fracturing occurred during processing.
7. Investigate the effects on ductility of finishing temperature during the latter stages of rolling. Reduced rolling temperatures were shown to produce a finer grain size in previous studies.

APPENDIX A

PROCESSING SCHEDULES

TABLE 8. PROCESSING SCHEDULE FOR 6061 AL USING 500°C INTERPASS ANNEALS (30 MINUTES).

Roll #	To (in)	Tf (in)	Mill Gap Setting (in)	Mill Deflect (in)	strain rate (1/sec)	e (in/in)
1	1.027	0.925	0.900	0.025	0.939	0.105
2	0.925	0.805	0.790	0.015	1.146	0.139
3	0.805	0.695	0.680	0.015	1.284	0.147
4	0.695	0.587	0.570	0.017	1.462	0.169
5	0.587	0.480	0.460	0.020	1.744	0.201
6	0.480	0.369	0.350	0.019	2.220	0.263
7	0.369	0.285	0.265	0.020	2.508	0.258
8	0.285	0.216	0.195	0.021	2.963	0.277
9	0.216	0.160	0.140	0.020	3.551	0.300
10	0.160	0.121	0.100	0.021	3.971	0.279
11	0.121	0.091	0.070	0.021	4.615	0.285
12	0.091	0.066	0.070	0.016	2.306	0.057
			Added Rolling Strain			2.480
			Total Strain			Unknown

TABLE 9. PROCESSING SCHEDULE FOR 6061 AL USING 500°C INTERPASS ANNEALS (5 MINUTES).

Roll #	To (in)	Tf (in)	Mill Gap Setting (in)	Mill Deflect (in)	strain rate (1/sec)	e (in/in)
1	1.027	0.927	0.900	0.027	0.929	0.102
2	0.927	0.812	0.790	0.022	1.116	0.132
3	0.812	0.702	0.680	0.022	1.252	0.146
4	0.702	0.591	0.570	0.021	1.469	0.172
5	0.591	0.484	0.460	0.024	1.731	0.200
6	0.484	0.375	0.350	0.025	2.176	0.255
7	0.375	0.285	0.265	0.020	2.570	0.274
8	0.285	0.219	0.195	0.024	2.884	0.263
9	0.219	0.166	0.140	0.026	3.380	0.277
10	0.166	0.129	0.100	0.029	3.692	0.252
11	0.129	0.090	0.070	0.020	5.068	0.360
12	0.090	0.065	0.070	0.015	2.332	0.057
			Total Rolling Strain			2.492
			Total Strain			Unknown

TABLE 10. PROCESSING SCHEDULE FOR 6061 AL - 10 V/O AL₂O₃ COMPOSITE USING 500°C INTERPASS ANNEALS (30 MINUTES) (HEAT I-1169).

Roll #	T ₀ (in)	T _f (in)	Mill Gap Setting (in)	Mill Deflect (in)	strain rate (1/sec)	e (in/in)
1	1.010	0.925	0.900	0.025	0.867	0.088
2	0.925	0.806	0.790	0.016	1.140	0.138
3	0.806	0.702	0.680	0.022	1.224	0.138
4	0.702	0.592	0.570	0.022	1.462	0.170
5	0.592	0.474	0.460	0.014	1.829	0.222
6	0.474	0.375	0.350	0.025	2.102	0.234
7	0.375	0.282	0.265	0.017	2.622	0.285
8	0.282	0.220	0.195	0.025	2.810	0.248
9	0.220	0.169	0.140	0.029	3.285	0.264
10	0.169	0.124	0.100	0.024	4.082	0.310
11	0.124	0.093	0.070	0.023	4.582	0.288
			Total Rolling Strain			2.385
Forging			max strain rate (1/sec)			
1	3.000	1.010		0.025		1.089
			Total Strain			3.474

TABLE 11. PROCESSING SCHEDULE FOR 6061 AL - 10 V/O AL₂O₃ COMPOSITE USING 500°C INTERPASS ANNEALS (5 MINUTES) (HEAT I-1169).

Roll #	T ₀ (in)	T _f (in)	Mill Gap Setting (in)	Mill Deflect (in)	strain rate (1/sec)	e (in/in)
1	1.010	0.928	0.900	0.028	0.850	0.085
2	0.928	0.815	0.790	0.025	1.104	0.130
3	0.815	0.698	0.680	0.018	1.291	0.155
4	0.698	0.596	0.570	0.026	1.409	0.158
5	0.596	0.478	0.460	0.018	1.816	0.221
6	0.478	0.378	0.350	0.028	2.095	0.235
7	0.378	0.289	0.265	0.024	2.530	0.268
8	0.289	0.218	0.195	0.023	2.969	0.282
9	0.218	0.161	0.140	0.021	3.554	0.303
10	0.161	0.124	0.100	0.024	3.819	0.261
11	0.124	0.093	0.070	0.023	4.582	0.288
			Total Rolling Strain			2.385
Forging			max strain rate (1/sec)			
1	3.000	1.010		.025		1.089
			Total Strain			3.474

TABLE 12. PROCESSING SCHEDULE FOR 6061 AL - 20 V/O AL₂O₃ COMPOSITE USING 500°C INTERPASS ANNEALS (30 MINUTES) (HEAT 1-1095).

Roll #	To (in)	Tf (in)	Mill Gap Setting (in)	Mill Deflect (in)	strain rate (1/sec)	e (in/in)
1	1.010	0.926	0.900	0.026	0.861	0.087
2	0.926	0.810	0.790	0.020	1.123	0.134
3	0.810	0.702	0.680	0.022	1.243	0.143
4	0.702	0.594	0.570	0.024	1.447	0.167
5	0.594	0.473	0.460	0.013	1.850	0.228
6	0.473	0.370	0.350	0.020	2.157	0.246
7	0.370	0.284	0.265	0.019	2.537	0.265
8	0.284	0.220	0.195	0.025	2.842	0.255
9	0.220	0.169	0.140	0.029	3.285	0.264
10	0.169	0.124	0.100	0.024	4.082	0.310
11	0.124	0.093	0.070	0.023	4.582	0.288
			Total Rolling Strain			2.385
Forging			max strain rate (1/sec)			
1	3.000	1.010		.025		1.089
			Total Strain			3.474

TABLE 13. PROCESSING SCHEDULE FOR 6061 AL - 20 V/O AL₂O₃ COMPOSITE USING 500°C INTERPASS ANNEALS (5 MINUTES) (HEAT 1-1095).

Roll #	To (in)	Tf (in)	Mill Gap Setting (in)	Mill Deflect (in)	strain rate (1/sec)	e (in/in)
1	1.100	0.920	0.900	0.020	1.197	0.179
2	0.920	0.821	0.790	0.031	1.037	0.114
3	0.821	0.703	0.680	0.023	1.287	0.155
4	0.703	0.595	0.570	0.025	1.445	0.167
5	0.595	0.480	0.460	0.020	1.792	0.215
6	0.480	0.374	0.350	0.024	2.159	0.250
7	0.374	0.285	0.265	0.020	2.560	0.272
8	0.285	0.223	0.195	0.028	2.777	0.245
9	0.223	0.163	0.140	0.023	3.577	0.313
10	0.163	0.124	0.100	0.024	3.890	0.273
11	0.124	0.094	0.070	0.024	4.491	0.277
			Total Rolling Strain			2.460
Forging			max strain rate (1/sec)			
1	3.000	1.027		0.025		1.072
			Total Strain			3.532

APPENDIX B

HARDNESS AND TENSILE TESTING RESULTS

TABLE 14. HARDNESS AND TENSILE DATA FOR 6061 AL - 30 MIN IPA AT 500°C

SHT TEMP 560 C							
TIME min	MEAN RH - °F	STD DEV	ERROR	YS (MPa)	UTS (MPa)	%Elong	Modulus (GPa)
0	32.7	1.53	2.80	54	188	34.4	65
10	69.0	2.02	3.70	119	253	29.4	62
24	79.2	0.53	0.98	153	277	26.1	61
56	88.2	1.54	2.83	210	317	23.7	60
133	92.4	0.63	1.15	249	334	21.3	75
316	95.5	0.49	0.89	275	343	21.4	86
750	96.8	0.54	0.98	282	350	18.9	70
1778	97.7	0.39	0.72	289	349	17.5	60
4217	97.6	0.45	0.82	291	343	17.4	64
10000	97.6	0.42	0.78	307	359	18.0	70
SHT TEMP 530 C							
TIME min	MEAN RH - °F	STD DEV	ERROR	YS (MPa)	UTS (MPa)	%Elong	Modulus (GPa)
0	28.4	3.93	7.21	97	180	29.2	xxxx
10	38.9	1.92	3.52	68	190	30.0	65
24	42.3	1.08	1.98	78	192	30.2	71
56	64.6	1.01	1.85	122	230	29.0	77
133	87.2	0.19	0.35	203	285	21.9	61
316	91.3	0.26	0.48	245	309	19.0	68
750	93.4	0.44	0.81	268	321	18.1	83
1778	94.1	0.35	0.64	262	320	17.0	xxxx
4217	93.5	0.43	0.78	270	319	18.4	65
10000	93.8	0.38	0.70	270	317	16.4	70
SHT TEMP 500 C							
TIME min	MEAN RH - °F	STD DEV	ERROR	YS (MPa)	UTS (MPa)	%Elong	Modulus (GPa)
0	19.3	2.49	4.57	50	160	31.5	59
10	19.4	1.88	3.45	51	165	32.5	xxxx
24	17.7	2.64	4.83	51	165	31.8	xxxx
56	22.4	2.00	3.67	56	167	31.3	xxxx
133	56.3	0.60	1.10	108	202	26.0	83
316	75.9	1.32	2.43	183	249	20.3	77
750	81.3	1.34	2.46	221	269	19.3	76
1778	83.5	0.77	1.41	226	271	18.5	76
4217	82.9	0.42	0.78	223	268	18.6	73
10000	81.8	1.30	2.39	228	270	18.6	76
SHT TEMP 480 C							
TIME min	MEAN RH - °F	STD DEV	ERROR	YS (MPa)	UTS (MPa)	%Elong	Modulus (GPa)
0	25.2	2.00	3.66	45	152	28.5	64
10	25.2	1.48	2.72	61	151	27.8	63
24	26.9	0.95	1.74	65	153	29.6	67
56	24.2	1.16	2.12	57	161	30.9	71
133	43.2	0.61	1.13	82	176	27.4	63
316	70.6	0.54	0.99	146	213	21.0	65
750	82.7	0.46	0.84	193	253	17.5	77
1778	82.7	0.71	1.31	204	255	16.1	85
4217	82.6	0.51	0.93	206	251	16.6	86
10000	82.6	1.07	1.96	201	254	17.5	69

TABLE 15. HARDNESS AND TENSILE DATA FOR 6061 AL - 5 MIN IPA AT 500°C

SHT TEMP 580 C							
TIME min	MEAN RH - °F	STD DEV	ERROR	YS (MPa)	UTS (MPa)	%Elong	Modulus (GPa)
0	32.7	2.52	4.63	54	181	31.5	68
10	69.5	0.55	1.01	113	245	28.4	59
24	79.8	0.79	1.44	154	276	27.9	60
56	88.3	0.99	1.81	202	300	24.0	73
133	93.0	0.50	0.92	221	319	19.7	71
316	97.0	0.58	1.06	256	344	19.3	64
750	94.5	1.45	2.66	283	343	19.5	70
1778	97.0	0.76	1.39	xxxx	351	17.7	xxxx
4217	98.8	0.31	0.57	280	334	18.8	64
10000	98.3	0.37	0.68	278	315	15.7	68
SHT TEMP 530 C							
TIME min	MEAN RH - °F	STD DEV	ERROR	YS (MPa)	UTS (MPa)	%Elong	Modulus (GPa)
0	31.2	1.82	3.34	55	181	32.4	xxxx
10	37.6	3.17	5.82	70	199	32.2	xxxx
24	50.8	1.45	2.66	62.5	213	31.2	78
56	73.1	0.69	1.27	136	255	25.3	69
133	90.1	0.47	0.86	215	300	22.1	68
316	92.8	1.02	1.88	252	319	21.4	81
750	93.5	0.71	1.30	268	327	16.8	80
1778	95.0	0.52	0.96	279	330	19.5	71
4217	94.3	0.80	1.46	276	330	18.5	71
10000	94.6	0.40	0.73	277	328	18.6	70
SHT TEMP 500 C							
TIME min	MEAN RH - °F	STD DEV	ERROR	YS (MPa)	UTS (MPa)	%Elong	Modulus (GPa)
0	21.5	1.61	2.96	50	166	30.7	97
10	21.6	2.88	5.27	49.5	167	32.5	83
24	23.6	1.09	2.00	48.5	165	28.9	63
56	29.0	2.16	3.98	xxxx	178	29.5	xxxx
133	64.9	0.44	0.81	131	224	25.4	74
316	81.3	0.42	0.78	xxxx	260	18.8	xxxx
750	85.5	0.46	0.85	233	279	18.5	81
1778	85.0	0.31	0.57	231	276	18.9	100
4217	85.0	0.41	0.76	xxxx	274	18.1	xxxx
10000	84.3	0.35	0.63	232	275	19.2	83
SHT TEMP 480 C							
TIME min	MEAN RH - °F	STD DEV	ERROR	YS (MPa)	UTS (MPa)	%Elong	Modulus (GPa)
0	14.8	3.34	6.12	58	152	32.1	xxxx
10	9.2	4.07	7.46	40.5	150	33.2	xxxx
24	12.4	4.25	7.79	40	147	32.7	xxxx
56	20.6	1.18	2.17	51	160	32.4	67
133	50.4	0.99	1.82	93	188	26.9	58
316	77.5	0.82	1.50	91.5	240	20.0	67
750	83.2	0.56	1.03	166	254	18.0	63
1778	83.4	0.44	0.81	201	262	18.4	81
4217	84.0	0.78	1.43	218	261	17.8	68
10000	82.9	0.45	0.83	215	256	16.6	76

TABLE 16. HARDNESS AND TENSILE DATA FOR 6061 AL - 10 V/O AL₂O₃ 30 MIN IPA AT 500°C

SHT TEMP 500 C							
TIME min	MEAN RH - °F	STD DEV	ERROR	YS (MPa)	UTS (MPa)	%Elong	Modulus (GPa)
0	68.8	1.63	2.99	136	253	21.0	80
10	73.0	4.27	7.82	154	282	19.8	xxxx
24	82.2	2.36	4.33	166	291	15.3	81
56	88.4	0.96	1.76	214	322	15.1	90
133	93.2	1.16	2.13	261	338	13.4	70
316	96.9	1.57	2.88	295	355	9.5	79
750	97.2	1.85	3.39	330	371	8.6	81
1778	98.1	1.86	3.41	344	399	8.0	85
4217	99.5	0.72	1.32	355	383	7.5	xxxx
10000	99.0	0.33	0.60	373	394	5.7	xxxx
SHT TEMP 530 C							
TIME min	MEAN RH - °F	STD DEV	ERROR	YS (MPa)	UTS (MPa)	%Elong	Modulus (GPa)
0	57.4	1.54	2.82	103	225	19.7	80
10	64.4	1.72	3.16	113	241	21.1	xxx
24	72.0	2.61	4.78	142	281	17.2	xxxx
56	88.4	0.69	1.26	214	301	9.1	xxxx
133	92.5	2.19	4.01	232	330	11.1	94
316	95.3	1.15	2.11	283	344	11.5	77
750	97.2	1.02	1.86	324	360	9.5	92
1778	97.1	0.79	1.45	334	366	6.1	75
4217	97.7	1.07	1.96	318	360	7.5	92
10000	97.4	0.56	1.02	333	362	8.4	92
SHT TEMP 500 C							
TIME min	MEAN RH - °F	STD DEV	ERROR	YS (MPa)	UTS (MPa)	%Elong	Modulus (GPa)
0	31.1	3.76	6.89	72	184	22.4	xxxx
10	39.7	1.22	2.24	71	193	21.7	xxxx
24	41.6	1.89	3.46	77	191	22.2	xxxx
56	59.1	1.39	3.65	117	218	17.7	xxxx
133	83.6	0.62	1.13	178	253	12.2	xxxx
316	92.4	0.47	0.86	270	308	11.0	84
750	91.5	0.84	1.54	266	318	9.0	91
1778	91.7	1.22	2.24	283	317	8.9	86
4217	90.3	0.89	1.63	279	309	7.7	86
10000	91.0	0.64	1.17	285	310	8.6	81
SHT TEMP 480 C							
TIME min	MEAN RH - °F	STD DEV	ERROR	YS (MPa)	UTS (MPa)	%Elong	Modulus (GPa)
0	17.0	5.37	9.85	65	165	22.2	89
10	25.1	4.32	7.91	68	167	20.4	xxxx
24	27.0	4.70	8.62	64	169	23.1	xxxx
56	33.4	1.77	3.24	65	173	22.6	xxxx
133	34.3	2.76	5.05	78	174	21.5	83
316	59.0	6.95	12.74	135	206	13.4	86
750	78.3	1.66	3.05	193	245	10.5	91
1778	81.8	0.48	0.88	214	255	9.3	83
4217	82.3	0.37	0.68	214	263	10.0	81
10000	78.9	0.57	1.06	209	255	9.0	78

TABLE 17. HARDNESS AND TENSILE DATA FOR 6061 AL - 10 V/O AL₂O₃ 5 MIN IPA AT 500°C

SHT TEMP 560 C							
TIME min	MEAN RH - °F	STD DEV	ERROR	YS (MPa)	UTS (MPa)	%Elong	Modulus (GPa)
0	59.9	0.56	1.03	131	261	14.9	75
10	79.6	0.85	1.56	166	294	16.3	80
24	84.0	0.53	0.97	171	304	15.6	83
58	91.3	0.75	1.37	237	338	14.6	88
133	95.3	0.35	0.65	282	357	10.9	88
316	97.5	0.31	0.56	311	377	8.8	83
750	98.8	0.34	0.62	326	374	9.7	83
1778	100.5	0.39	0.72	349	386	7.8	85
4217	99.9	0.45	0.83	359	383	3.2	76
10000	97.3	0.48	0.88	351	376	6.0	76
SHT TEMP 530 C							
TIME min	MEAN RH - °F	STD DEV	ERROR	YS (MPa)	UTS (MPa)	%Elong	Modulus (GPa)
0	50.7	1.33	2.44	97	218	19.5	xxxx
10	61.3	1.51	2.76	109	238	20.5	97
24	66.7	1.40	2.57	123	244	15.1	97
56	82.8	1.14	2.10	182	284	17.3	79
133	91.0	0.60	1.10	248	315	7.9	79
316	96.5	0.44	0.81	289	344	11.4	88
750	95.2	0.79	1.45	xxxx	xxxx	xxxx	xxxx
1778	98.0	0.44	0.81	312	349	7.6	xxxx
4217	96.7	0.50	0.91	xxxx	344	4.6	xxxx
10000	96.0	0.63	1.15	310	339	8.5	78
SHT TEMP 500 C							
TIME min	MEAN RH - °F	STD DEV	ERROR	YS (MPa)	UTS (MPa)	%Elong	Modulus (GPa)
0	35.5	1.91	3.50	88	187	22.6	70
10	34.7	3.83	7.02	91	183	22.5	83
24	44.1	0.70	1.28	98	190	20.2	79
56	59.7	1.10	2.02	135.5	215	17.9	71
133	83.9	1.22	2.24	228	275	11.1	93
316	93.1	0.39	0.71	296	309	8.6	101
750	92.8	0.82	1.50	295	316	8.7	92
1778	92.1	1.10	2.02	263	321	8.6	92
4217	92.0	1.16	2.13	288	318	8.4	83
10000	91.4	0.70	1.28	270	297	7.1	79
SHT TEMP 480 C							
TIME min	MEAN RH - °F	STD DEV	ERROR	YS (MPa)	UTS (MPa)	%Elong	Modulus (GPa)
0	29.4	2.92	5.36	73	180	21.8	xxxx
10	33.6	2.63	4.82	82	172	11.6	xxxx
24	33.3	1.89	3.47	67	173	18.1	83
56	34.7	2.22	4.07	68	173	18.0	88
133	57.7	0.74	1.35	107	207	17.7	83
316	78.0	1.37	2.51	183	251	11.2	xxx
750	85.3	0.25	0.46	239	277	7.9	91
1778	85.8	1.58	2.89	253	287	8.4	89
4217	89.1	1.82	3.34	250	283	7.9	83
10000	85.0	0.41	0.76	238	267	9.0	xxxx

TABLE 18. HARDNESS AND TENSILE DATA FOR 6061 AL - 20 V/O AL₂O₃ 30 MIN IPA AT 500°C

SHT TEMP 500 C							
TIME min	MEAN RH - °F	STD DEV	ERROR	YS (MPa)	UTS (MPa)	%Elong	Modulus (GPa)
0	72.9	1.88	3.45	148	268	9.2	86
10	80.1	1.25	2.29	180	288	10.6	89
24	81.7	2.69	4.93	188	292	6.4	91
56	91.7	3.04	5.57	248	313	3.6	103
133	95.3	3.03	5.55	289	361	6.27	97
316	100.5	1.00	1.84	326	383	3.5	xxxx
750	99.3	1.51	2.77	358	395	1.9	93
1778	101.2	1.49	2.73	384	402	3.1	89
4217	100.8	2.06	3.78	396	416	2.9	89
10000	100.7	0.82	1.51	356	381	0.9	xxxx
SHT TEMP 530 C							
TIME min	MEAN RH - °F	STD DEV	ERROR	YS (MPa)	UTS (MPa)	%Elong	Modulus (GPa)
0	69.7	1.04	1.90	126	252	13.0	91
10	70.1	1.48	2.71	125	244	13.3	89
24	76.7	0.79	1.44	150	262	10.4	80
56	92.7	0.91	1.67	240	317	6.2	92
133	97.0	0.35	0.65	300	356	4.0	81
316	99.8	1.00	1.83	343	375	2.4	95
750	99.3	0.53	0.97	346	376	3.9	98
1778	99.9	1.17	2.14	364	392	3.0	98
4217	100.1	0.48	0.88	356	382	2.7	95
10000	99.6	0.59	1.08	352	381	2.4	93
SHT TEMP 500 C							
TIME min	MEAN RH - °F	STD DEV	ERROR	YS (MPa)	UTS (MPa)	%Elong	Modulus (GPa)
0	50.6	1.58	2.90	92	192	14.5	88
10	48.7	2.23	4.09	88	193	16.1	88
24	45.5	2.79	5.12	88	195	17.3	83
56	58.2	1.27	2.33	108	210	14.2	88
133	78.7	1.48	2.71	185	254	8.9	87
316	90.7	1.18	2.16	267	302	4.0	86
750	94.2	0.30	0.55	296	321	4.8	100
1778	92.8	1.25	2.29	285	312	2.7	92
4217	94.4	0.97	1.78	290	318	4.2	92
10000	93.9	0.20	0.36	285	321	4.6	97
SHT TEMP 480 C							
TIME min	MEAN RH - °F	STD DEV	ERROR	YS (MPa)	UTS (MPa)	%Elong	Modulus (GPa)
0							
10							
24							
56							
133							
316							
750							
1778							
4217							
10000							

TABLE 19. HARDNESS AND TENSILE DATA FOR 6061 AL - 20 V/O AL₂O₃ 5 MIN IPA AT 500°C

SHT TEMP 500 C							
TIME min	MEAN RH - °F	STD DEV	ERROR	YS (MPa)	UTS (MPa)	%Elong	Modulus (GPa)
0	71.6	1.80	3.29	149	263	9.7	103
10	83.4	1.45	2.66	172	280	6.1	100
24	84.7	1.01	1.85	182	287	6.0	89
56	93.6	0.99	1.81	263	342	5.7	107
133	99.3	0.41	0.76	288	353	2.6	88
316	98.8	1.08	1.98	308	377	2.4	97
750	102.0	0.42	0.77	324	398	2.7	101
1778	101.5	0.37	0.68	325	395	1.4	103
4217	101.3	0.34	0.62	364	396	1.7	93
10000	100.8	0.57	1.04	336	366	1.4	97
SHT TEMP 530 C							
TIME min	MEAN RH - °F	STD DEV	ERROR	YS (MPa)	UTS (MPa)	%Elong	Modulus (GPa)
0	65.7	1.24	2.27	128	247	11.3	91
10	75.2	0.81	1.49	139	259	12.5	91
24	78.9	1.12	2.60	158	272	12.9	91
56	88.5	1.21	2.22	215	307	7.8	89
133	96.2	0.48	0.88	290	321	1.9	95
316	98.7	1.11	2.04	323	357	2.4	95
750	99.2	0.72	1.32	323	371	3.1	93
1778	99.7	0.65	1.19	342	386	3.1	108
4217	99.2	0.96	1.75	344	377	4.1	94
10000	98.8	0.68	1.24	329	361	1.1	101
SHT TEMP 500 C							
TIME min	MEAN RH - °F	STD DEV	ERROR	YS (MPa)	UTS (MPa)	%Elong	Modulus (GPa)
0	45.9	2.45	4.49	67.5	190	8.9	xxxx
10	51.4	1.95	3.57	66	194	11.1	83
24	55.9	1.08	1.98	64	203	13.3	77
56	69.7	0.99	1.81	71	223	6.7	xxxx
133	88.4	0.93	1.71	94	284	3.8	xxxx
316	95.6	0.43	0.78	217	318	1.1	81
750	96.1	0.56	1.02	221	333	2.7	86
1778	95.2	0.43	0.79	230	330	1.8	xxxx
4217	95.6	0.59	1.08	243	333	3.4	81
10000	93.5	1.10	2.02	294	345	2.6	100
SHT TEMP 480 C							
TIME min	MEAN RH - °F	STD DEV	ERROR	YS (MPa)	UTS (MPa)	%Elong	Modulus (GPa)
0	41.6	3.34	6.13	89	185	11.3	88
10	46.3	1.07	1.96	94	193	12.4	86
24	46.6	1.94	3.56	94	190	10.2	83
56	46.2	1.33	2.43	96	191	10.2	94
133	69.1	0.59	1.08	143	223	6.9	83
316	84.3	1.24	2.27	215	275	3.2	76
750	88.6	1.04	1.90	259	291	2.5	94
1778	90.6	0.76	1.39	267	299	5.9	95
4217	87.4	0.57	1.05	263	300	482.0	93
10000	86.9	1.64	3.01	257	285	4.2	91

APPENDIX C

GRAPHICAL PRESENTATION

OF HARDNESS AND TENSILE

TEST DATA

FOR 5 MIN IPA AT 500°C

6061 Aluminum 5 min IPA at 500C

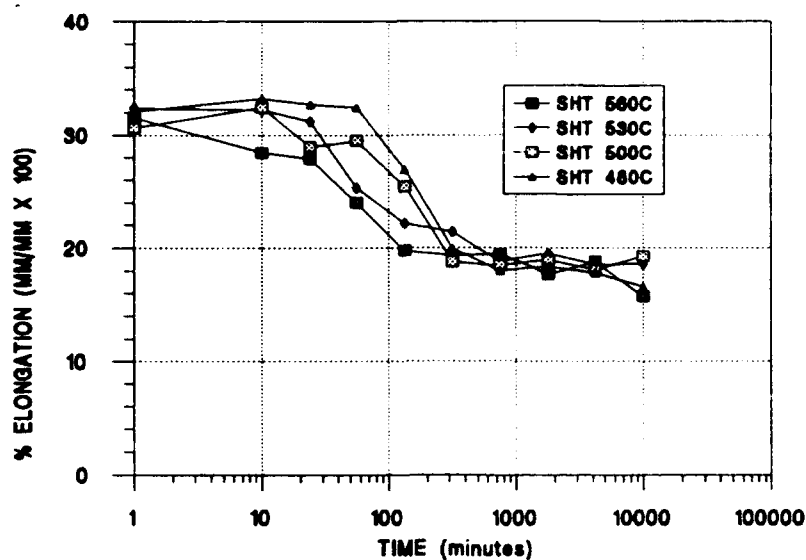


Figure 46. Plot of elongation versus aging time for unreinforced 6061 material processed utilizing a 5 min. IPA during rolling at 500°C. Data are included for four different solution heat treatment temperatures.

6061 Aluminum 5 min IPA at 500C

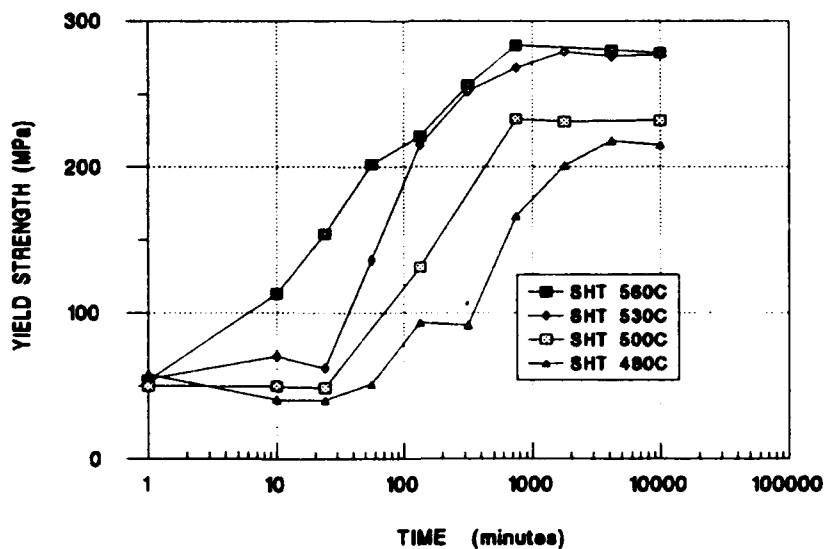


Figure 47. Plot of yield strength versus aging time for unreinforced 6061 material processed utilizing a 5 min. IPA during rolling at 500°C. Data are included for four different solution heat treatment temperatures.

6061 Al 5 min IPA at 500C

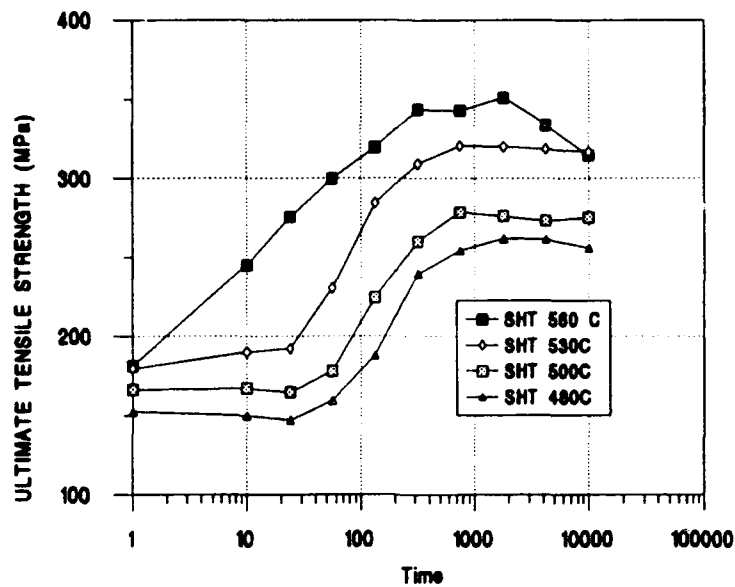


Figure 48. Plot of ultimate tensile strength versus aging time for unreinforced 6061 material processed utilizing a 5 min. IPA during rolling at 500°C. Data are included for four different solution heat treatment temperatures.

6061 Aluminum 5 min IPA at 500C

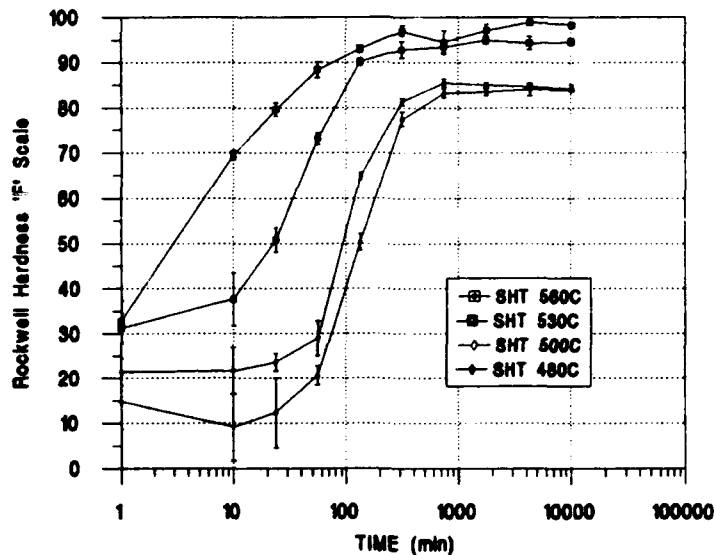


Figure 49. Plot of hardness versus aging time for unreinforced 6061 material processed utilizing a 5 min. IPA during rolling at 500°C. Data are included for four different solution heat treatment temperatures.

6061 Al - 10 v/o Al₂O₃ 5 min IPA at 500C

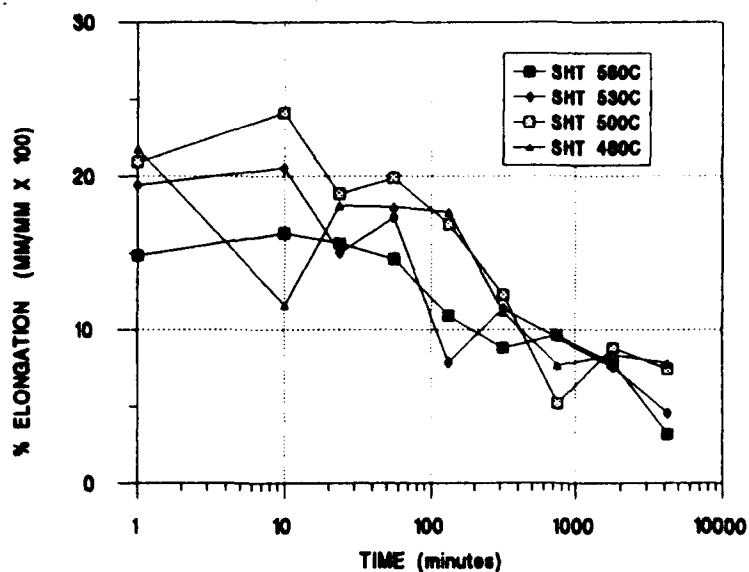


Figure 50. Plot of elongation versus aging time for 6061 Al - 10 vol. pct. Al₂O₃ material processed utilizing a 5 min. IPA during rolling at 500°C. Data are included for four different solution heat treatment temperatures.

6061 Al - 10 v/o Al₂O₃ 5 min IPA at 500C

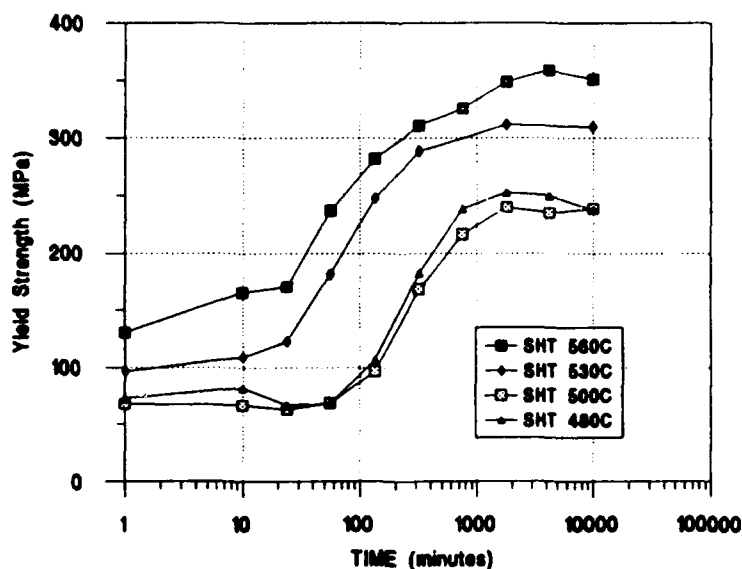


Figure 51. Plot of yield strength versus aging time for 6061 Al - 10 vol. pct. Al₂O₃ material processed utilizing a 5 min. IPA during rolling at 500°C. Data are included for four different solution heat treatment temperatures.

6061 Al -10 v/o Al₂O₃ 5 min IPA at 500C

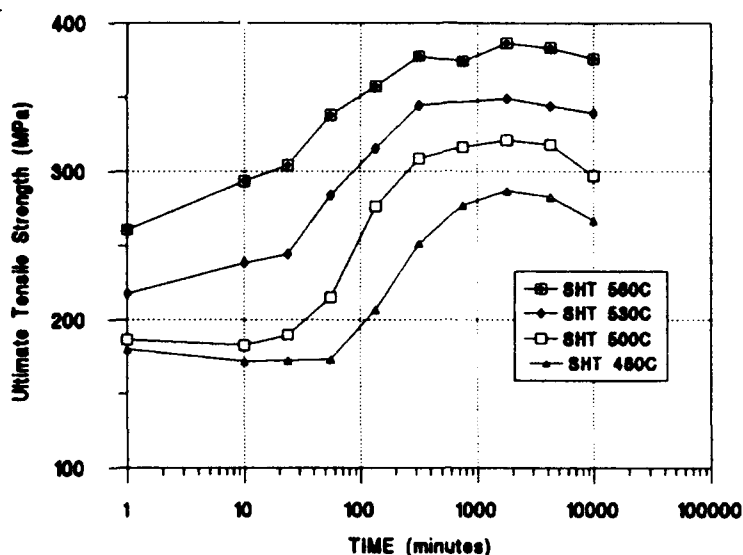


Figure 52. Plot of ultimate tensile strength versus aging time for 6061 Al - 10 vol. pct. Al₂O₃ material processed utilizing a 5 min. IPA during rolling at 500°C. Data are included for four different solution heat treatment temperatures.

6061 Al - 10 v/o Al₂O₃ 5 min IPA at 500C

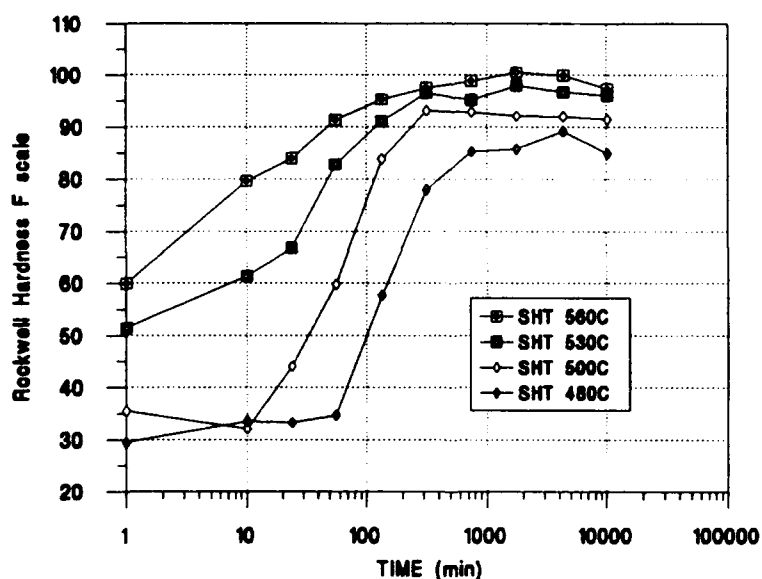


Figure 53. Plot of hardness versus aging time for 6061 Al - 10 vol. pct. Al₂O₃ material processed utilizing a 5 min. IPA during rolling at 500°C. Data are included for four different solution heat treatment temperatures.

6061 Al - 20 v/o Al₂O₃ 5 min IPA at 500C

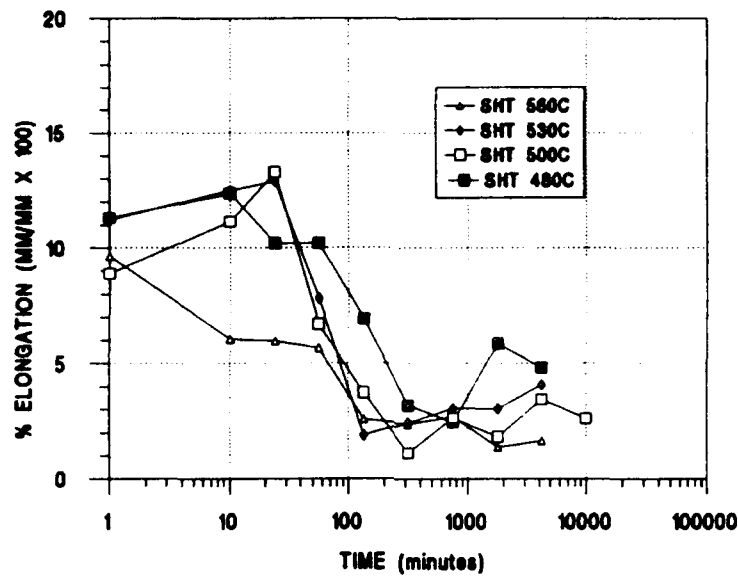


Figure 54. Plot of elongation versus aging time for 6061 Al - 20 vol. pct. Al₂O₃ material processed utilizing a 5 min. IPA during rolling at 500°C. Data are included for four different solution heat treatment temperatures.

6061 Al - 20 v/o Al₂O₃ 5 min IPA at 500C

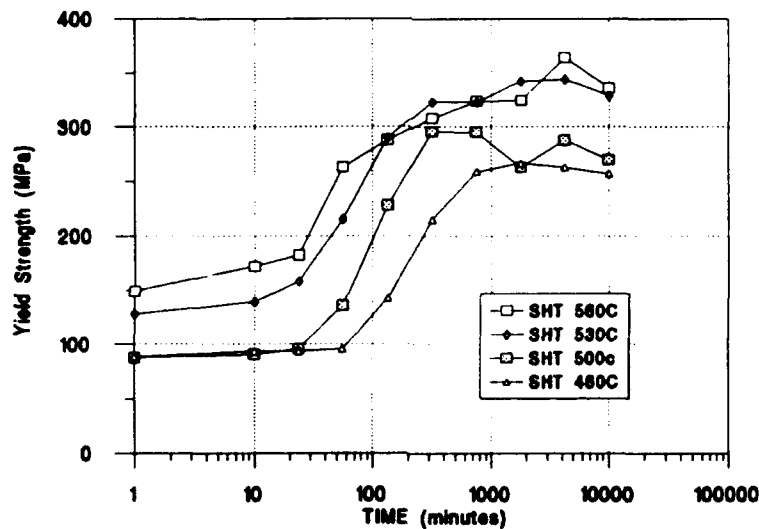


Figure 55. Plot of yield strength versus aging time for 6061 Al - 20 vol. pct. Al₂O₃ material processed utilizing a 5 min. IPA during rolling at 500°C. Data are included for four different solution heat treatment temperatures.

6061 Al - 20 v/o Al₂O₃ 5 min IPA at 500C

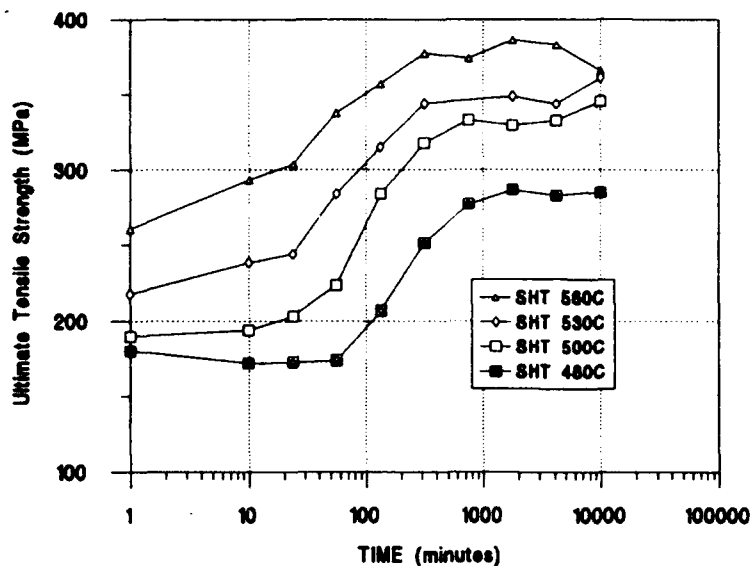


Figure 56. Plot of ultimate tensile strength versus aging time for 6061 Al - 20 vol. pct. Al₂O₃ material processed utilizing a 5 min. IPA during rolling at 500°C. Data are included for four different solution heat treatment temperatures.

6061 Al - 20 v/o Al₂O₃ 5 min IPA at 500C

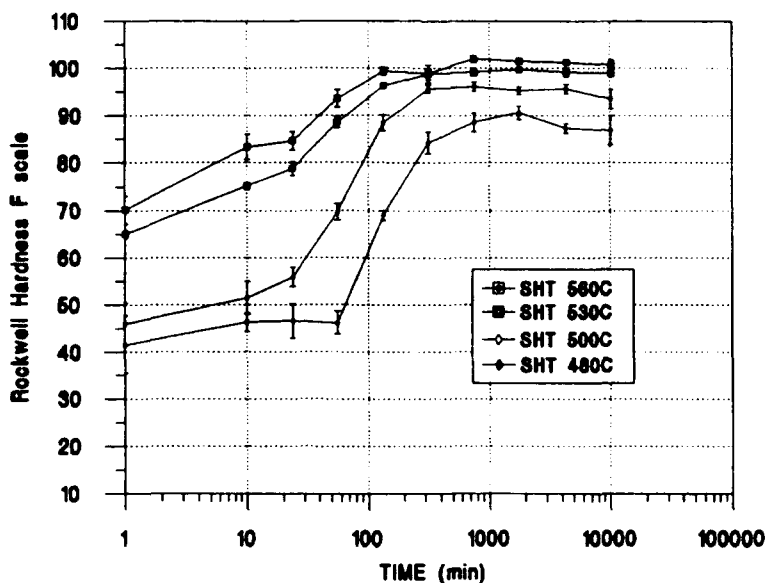


Figure 57. Plot of hardness versus aging time for 6061 Al - 20 vol. pct. Al₂O₃ material processed utilizing a 5 min. IPA during rolling at 500°C. Data are included for four different solution heat treatment temperatures.

REFERENCES

1. Cooperative Research and Development Agreement -- Naval Postgraduate School/DURALCAN-USA Cooperative Research in Thermomechanical Processing and Ductility Enhancement of DURALCAN Composite Materials, April 1993.
2. McNelley, T. R., Crooks, R., Kalu, P. N., and Rogers, S. A., "Precipitation and Recrystallization During Processing of a Superplastic Al-10Mg-0.1Zr alloy", *Materials Science and Engineering*, A166 pp. 135-143 (1993).
3. Hales S. J., McNelley, T. R., and McQueen, H. J., *Metallurgical Transactions. A*, Vol. 22, p. 1037 (1991).
4. Hales S. J. and McNelley, T. R., in H. C. Heikkinen and T.R. McNelley (eds.), *Proc Symp. on Superplasticity in Aerospace*, TMS, Warrendale PA p. 61, (1988).
5. Crooks, R., Hales, S. J., and McNelley, T. R. in C. H. Hamilton and N. E. Paton (eds.), *Superplasticity and Superplastic Forming*, TMS, Warrendale PA p. 389, (1988).
6. McNelley, T. R., and Kalu, P. N. in S. Hori, M. Tokizane and N. Furushiro (eds.) *Proc. of Superplasticity in Advanced Materials*, JSRS, Osaka University, Osaka, Japan, p. 413 (1991).
7. Hales, S. J., McNelley, T. R., and Crooks, R., in T. Chandra (ed.), *Recrystallization '90, Proc. Int. Conf.*, TMS, Warrendale PA p. 231 (1990).
8. Gorsuch, T.E., *The Roles of Strain and Reheating Interval in the Continuous Recrystallization During Thermomechanical Processing by Warm Rolling of an Al-Mg Alloy*, Master's Thesis, Naval Postgraduate School, December 1989.
9. Rogers, S.A., *The Roles of Particles in Recrystallization of a Thermomechanically Processed Al-Mg Alloy*, Master's Thesis, Naval Postgraduate School, September 1992.
10. Kalu and T. R. McNelley, "Microstructural Refinement by Thermomechanical Treatment of a Cast and Extruded Al-Al₂O₃ Composite", *Scripta Metallurgica et Materialia*, Pergamon Press, Vol. 25, pp. 853-858, (1991).
11. McNelley, T. R., and Kalu, P.N., "The Effects of Thermomechanical Processing on the Ambient Temperature Properties and Aging Response of a 6061 Al-Al₂O₃ Composite", *Scripta Metallurgica et Materialia* Pergamon Press, Vol. 25, pp. 1041-1046, (1991).
12. McNelley, T.R. and Kalu, P.N., "Thermomechanical Processing and Ductility Enhancement of a 6061 Al - Al₂O₃ Metal Matrix Composite", *Advanced Synthesis of Engineered Structural Materials*, Proceeding of the International Conference, San Francisco, CA, USA 30 August-2 September 1992, ASM International, Materials Park, OH.
13. Schaefer, T. A., *Thermomechanical Processing and Ambient Temperature Properties of a 6061 Aluminum 10 Volume Percent Alumina Metal Matrix Composite*, Master's Thesis, Naval Postgraduate School, p. 13, March 1990.

14. Macri, P.D., *Processing Microstructure and Elevated Temperature Mechanical Properties of a 6061 Aluminum-Alumina Metal Matrix Composite*, Master's Thesis, Naval Postgraduate School, December 1990.
15. Magill, M. D., *The Influence of Thermomechanical Processing Parameters on the Elevated Temperature Mechanical Behavior of a 6061 Aluminum-Alumina Metal Matrix Composite Materials*, Master's Thesis, Naval Postgraduate School, December 1990.
16. Schauder, T. J., *The Elevated Temperature Behavior of a 10% Volume Al-Al₂O₃ Metal-Matrix Composite*, Master's Thesis, Naval Postgraduate School, March 1992.
17. Eastwood, D.F., *The Effect of Thermomechanical Processing Parameters on the Ambient Behavior of 10% Volume Al-Alumina*, Master's Thesis, Naval Postgraduate School, March 1992.
18. Osman, T. M., Lewandowski, J. J. and Hunt Jr., W. H., "Different Deformation Histories", *Fabrication of Particulates Reinforced Composites*, pp. 209-116, ASM International Conference Proceedings, 1990
19. Lewandowski, J. J. et al., "Effects of Casting Conditions and Deformation Processing on A356 Aluminum and A356-20 Vol. % SiC Composites", *Journal of Composite Materials* Vol. 26, No. 14, pp. 2076-2106, (1992).
20. Llorca, J., Needleman, A., et al., "An Analysis of the Effects of Matrix Void Growth on Deformation and Ductility in Metal-Ceramic Composites", *Acta metall. mater.*, Pergamon Press, Vol. 39 No. 10, pp. 2317-2335, (1991).
21. Longenecker, F. W., "An Analysis of the Microstructure and Reinforcement Distribution of an Extruded Particle- Reinforced Al 6061 10 v/o Percent Al₂O₃ Metal Matrix Composite ", Master's Thesis, Naval Postgraduate School, September 1993.
22. Humphreys, F. J., "The Nucleation of Recrystallization at Second Phase Particles in Deformed Aluminum", *ACTA METALLURGICA.*, Pergamon Press, Vol. 25, pp. 1323 (1977)
23. Humphreys, F. J. and Kalu, P. N., "Dislocation-Particle interactions During High Temperature Deformation of Two-Phase Aluminium Alloys", *ACTA METALLURGICA.*, Pergamon Press, Vol. 35, pp. 2815 (1987)
24. Humphreys, F. J. and Kalu, P. N., in *Aluminum Technology '86*, Institute of Metals, London, 1986, p.347.
25. Humphreys, F. J. and Miller, W. S. et al., "Microstructural Developement During Thermomechanical Processing of Particulate Metal Matrix Composites", *Materials Science and Technology*, Vol. 6, pp. 1157-1166, November 1990.
26. Dixon, W. , DURACAN-USA, San Diego, CA Private Communication.
27. Dixon, W. , DURACAN-USA, San Diego, CA Private Communication.
28. Dieter, George, *Mechanical Metallurgy, 2nd Edition*, (International Student Edition), McGraw Hill, p 633 , (1976).

29. *Metals Handbook*, Tenth Edition, Volume 2, edited by Davis, Joseph R., et al., pp. 103-104, ASM International (1990).
30. Ingalls, A.G, *Amateur Telescope Making*, Scientific American, Inc. NY 1970.
31. Gysler, A. et al., "A Comparison of Microstructure and Tensile Properties of P/M and I/M Al-Li-X Alloys", *Aluminum-Lithium Alloys AIME Conference Proceedings* Sanders, T. H. and Starke, E. A. Jr. (eds.) pp. 265 , (1980)

INITIAL DISTRIBUTION LIST

	No Copies
1. Library, Code 52 411 Dyer Rd. Rm 104 Naval Postgraduate School Monterey, CA 93943-5101	2
2. Defense Technical Information Center Cameron Station Alexandria, VA 22304-6145	2
3. Mr. William Dixon Director, Extrusion Development DURALCAN-USA 10505 Roselle Street San Diego, CA 92121	2
3. Chairman, Code ME/Kk Mechanical Engineering Department Naval Postgraduate School Monterey, CA 93943-5108	1
4. Professor T. McNelley, Code ME/Mc Mechanical Engineering Department Naval Postgraduate School Monterey, CA 93943-5108	5
5. Naval Engineering Curricular Officer, Code 34 Mechanical Engineering Department Naval Postgraduate School Monterey, CA 93943-5109	1
6. LCDR Werner Hoyt, USN Executive Officer SUPSHIP Long Beach Long Beach, CA 90822	2